Mobile-station and Base-station Cooperation

Presented by
Lajos Hanzo
School of Electronics and Computer Science,
University of Southampton, SO17 1BJ, UK.
http://www-mobile.ecs.soton.ac.uk

Acknowledgements

- Sincere thanks are due to the team back at 'base' in Southampton, in particular to Lie-Liang Yang, Soon-Xin Ng, Wei Fang, Nan Wu, Rong Zhang, Lingkun Kong, Li Wang, Fasih Butt, Mohammed El-Hajjar, KyungChun Lee, SeungHwan Won, Shinya Sugiura.
- The Sponsors: EPSRC, the EU, the VCE
- **Background Reading:**
  L. Hanzo, O. Alamri, M. El-Hajjar, N. Wu: Near-Capacity Multi-Functional MIMO Systems: Sphere-Packing, Iterative Detection and Cooperation, IEEE Press - John Wiley, 2009

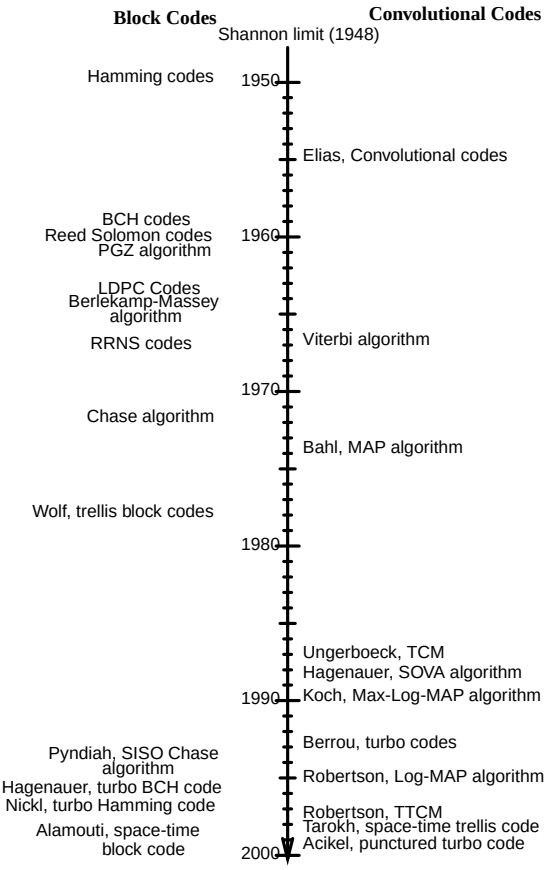

Figure 1: A glimpse of post-Shannon history

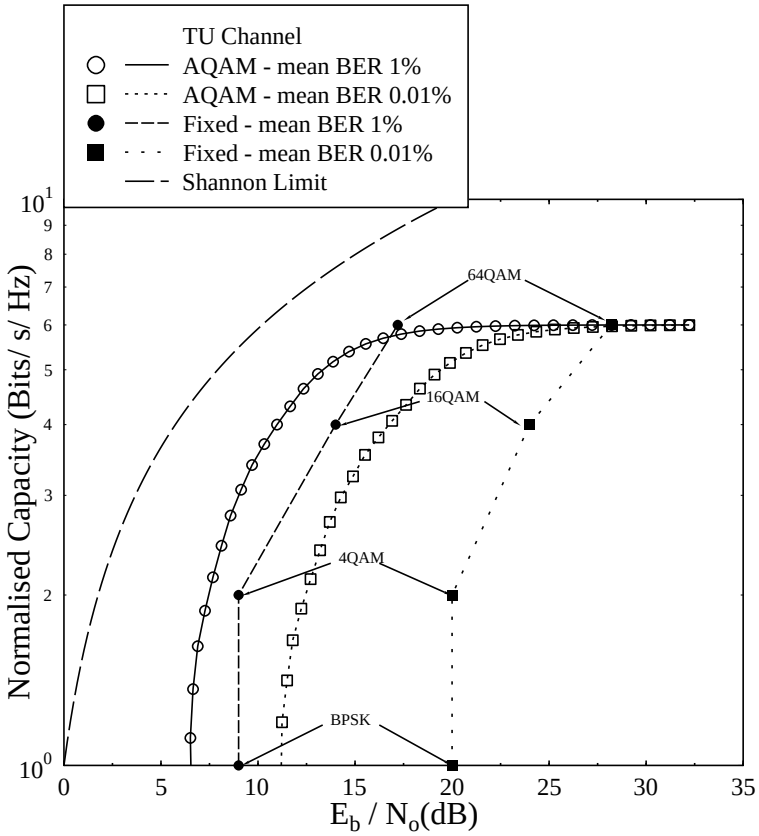

Figure 2: Channel capacity upper bound of HSDPA-style AQAM and fixed modulation schemes over the COST 207 TU Rayleigh Fading channel for BER=1% and BER=0.01%.

Averting the WWW: MIMOs, Cooperative Communications and Transmit Preprocessing

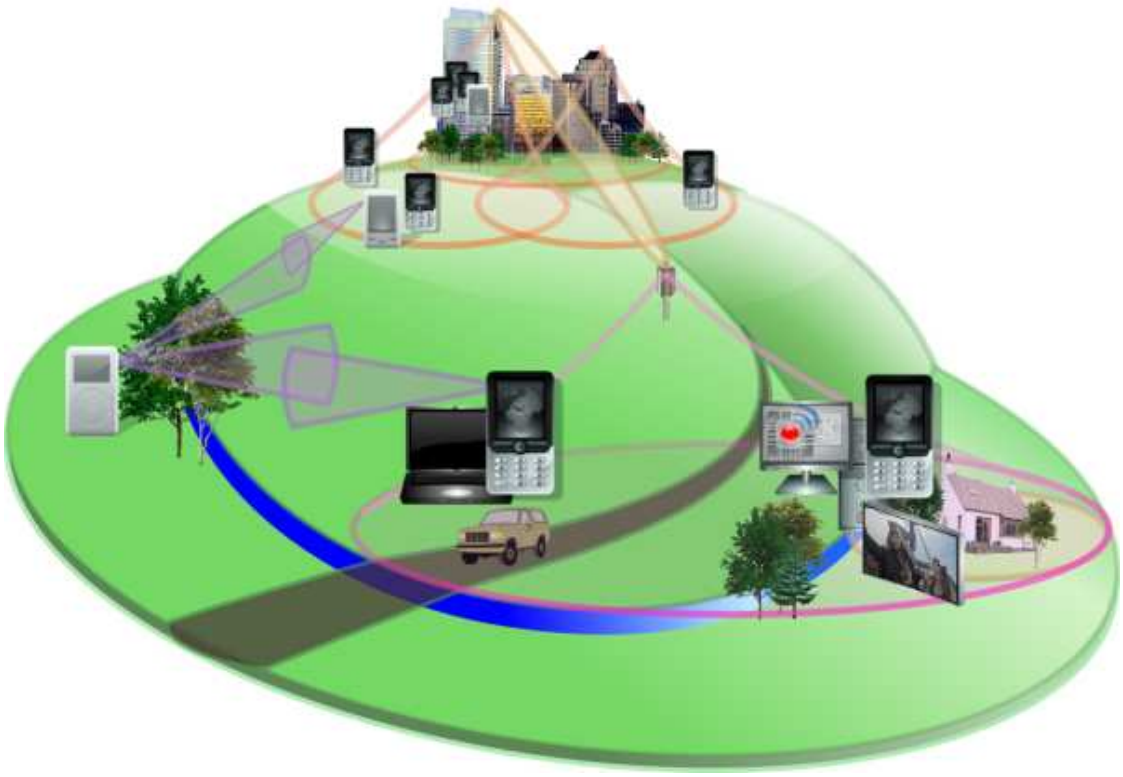

Capacity of MIMOs

$$C \approx min(M; N)$$

- *The classic Shannon-Hartley law suggests that the achievable channel capacity increases logarithmically with the transmit power.*
- *By contrast, the MIMO capacity increases linearly with the number of transmit antennas, provided that the number of receive antennas is equal to the number of transmit antennas. With the further proviso that the total transmit power is increased proportionately to the number of transmit antennas, a linear capacity increase is achieved upon increasing the transmit power, which justifies the spectacular success of MIMOs...*
- **L. Hanzo, O. Alamri, M. El-Hajjar, N. Wu**: Near-Capacity Multi-Functional MIMO Systems; *John Wiley and IEEE PRESS*, 2009

Capacity of MIMO Systems

Discrete-Input Continuous-Output Memoryless Channel (DCMC)

- The Full-multiplexing-gain system has a higher asymptotic capacity as a benefit of its multiplexing gain.
- The gap between the capacity curves of the Rayleigh fading channel and the AWGN channel is narrower for the full-diversity system as a benefit of its diversity gain.

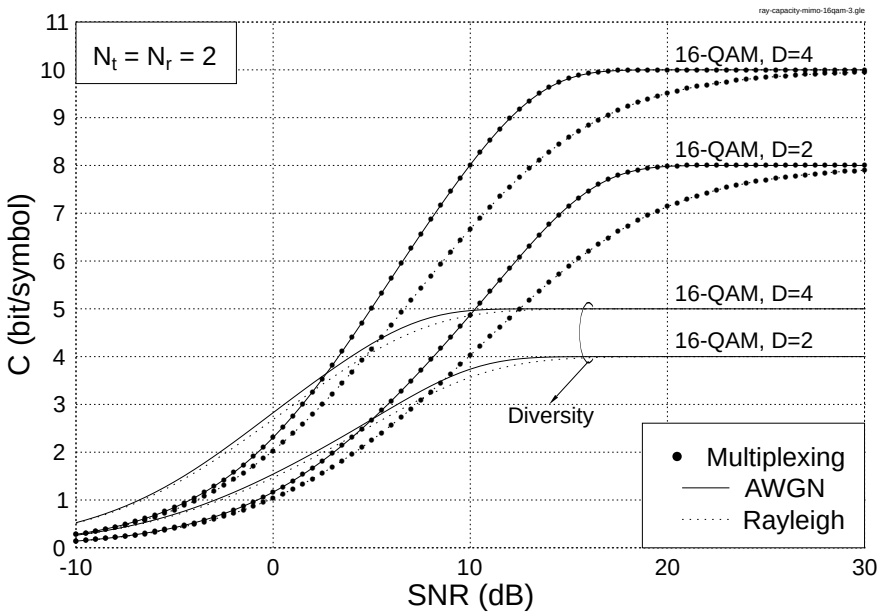

The capacity of $D = 2$ and 4 dimensional 16QAM-based MIMO DCMC uncorrelated Rayleigh-fading channel and AWGN channel.

Evolution of the Four MIMOs in Wireless Communications

- Type I: Beamforming
- Type II - SDMA: Spatial Division Multiple Access
- Type III - SDM: Spatial Division Multiplexing
- Type IV - Space-Time Coding: STTC, STBC and STS

Type I MIMOs: Beamforming

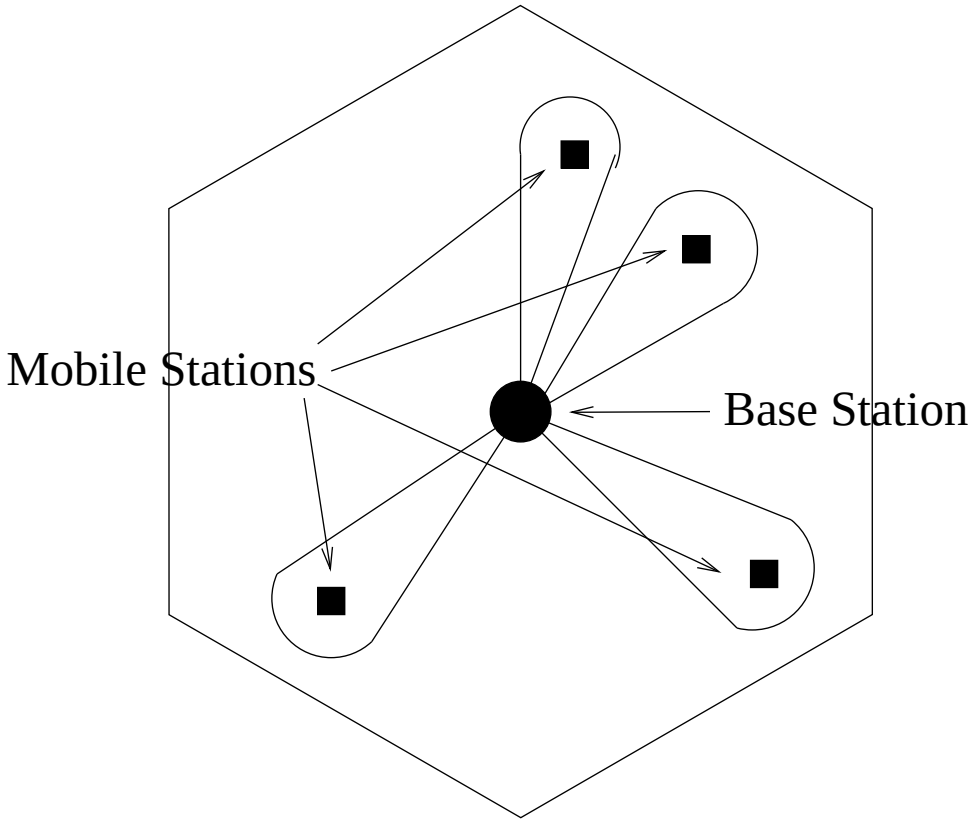

Multiple Antenna Aided Spatial Division Multiple Access OFDM

Type II MIMOs: SDMA

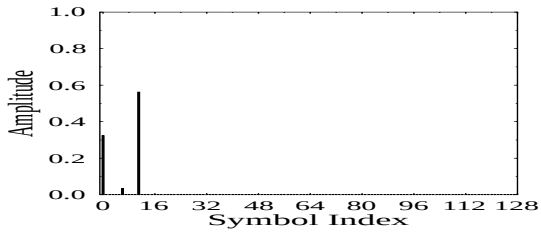

(a) CIR 1: user 1, antenna 1

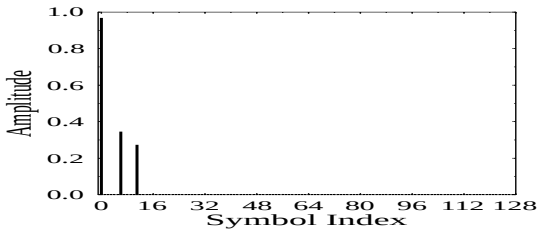

(b) CIR 2: user 1, antenna 2

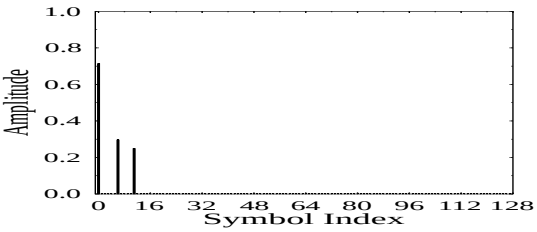

(c) CIR 3: user 2, antenna 1

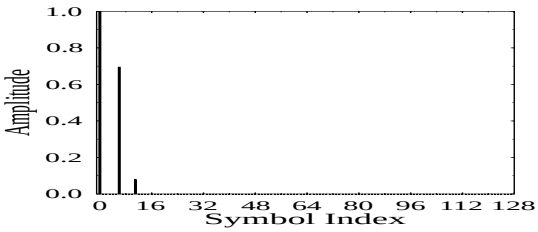

(d) CIR 4: user 2, antenna 2

Figure 3: Evolution from CDMA to SDMA: Four different channel impulse responses (CIR) recorded at the two receiver antennas for the two users supported.

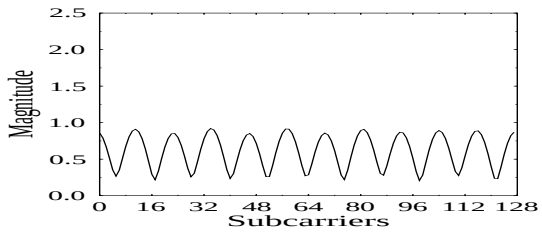

(a) CTF 1: user 1, antenna 1

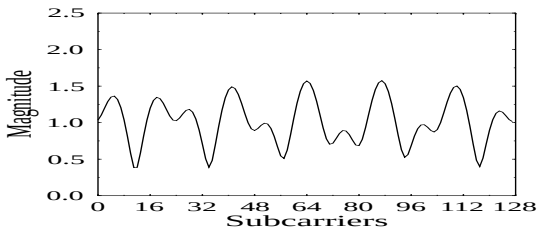

(b) CTF 2: user 1, antenna 2

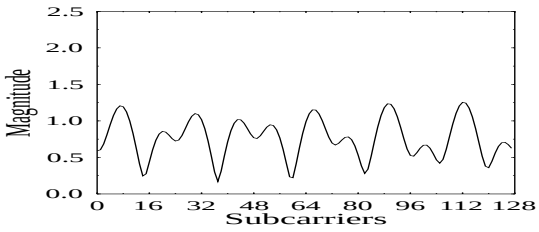

(c) CTF 3: user 2, antenna 1

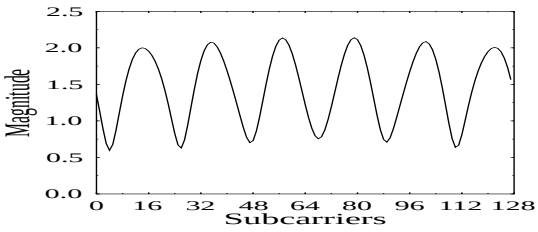

(d) CTF 4: user 2, antenna 2

Figure 4: Channel transfer functions (CTF) for the CIRs seen in Figure 3 (a) CTF 1, (b) CTF 2, (c) CTF 3, and (d) CTF 4.

Type III MIMOs: SDM ML Sphere-Detector for Rank-Deficient Scenarios

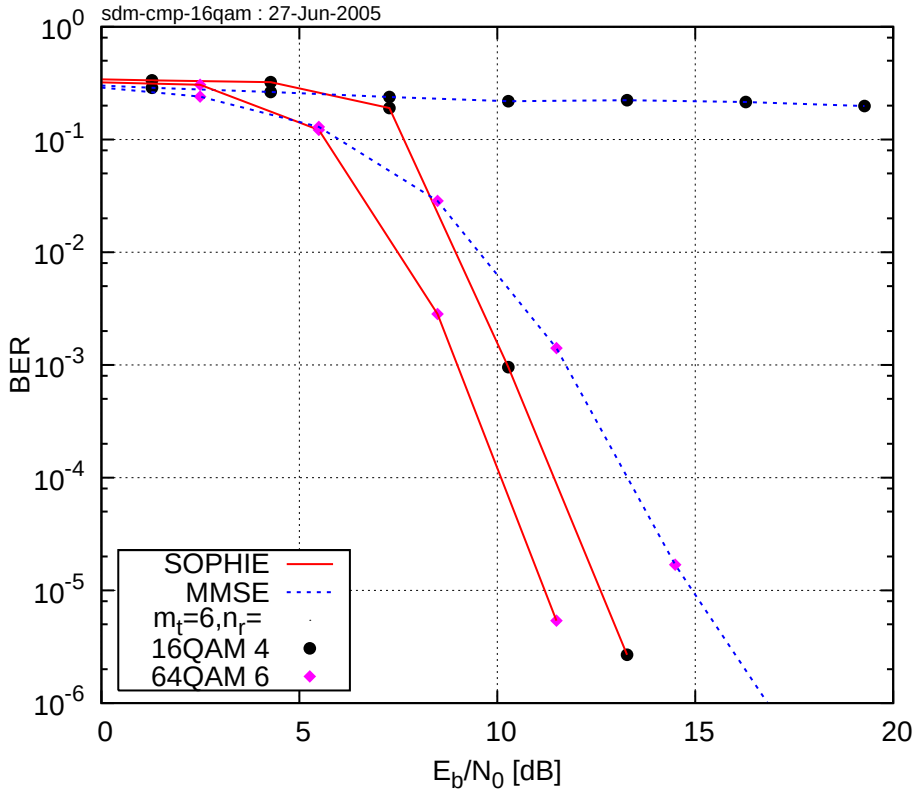

- The proposed SOPHIE SDM detection method exhibits near-optimum performance and relatively low complexity in high-throughput scenarious such as 6x6 64QAM as well as rank-deficient 6x4 16QAM MIMO-OFDM. **The throughput is 36 and 24 bits/symbol, respectively.**

Channel Variation in Space-Time Coded OFDM: Type IV MIMO

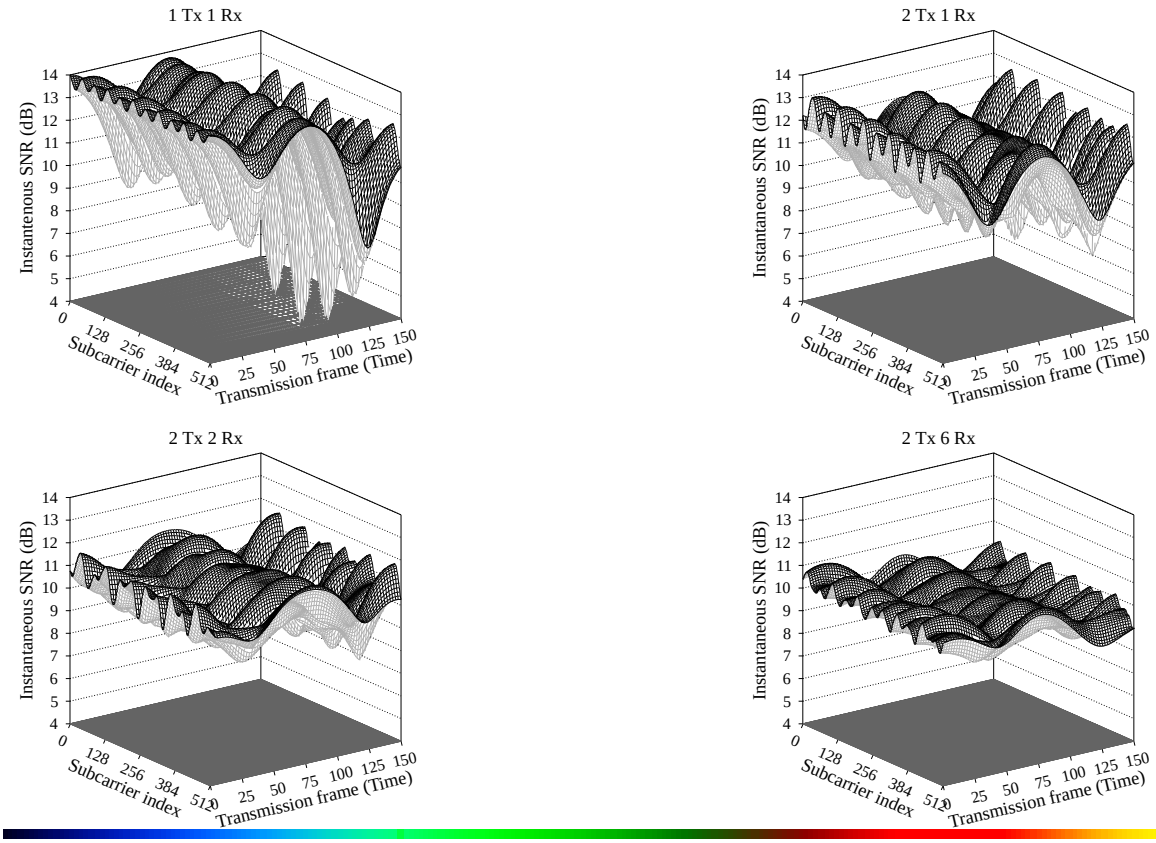

Near-Instantaneously Adaptive Cooperative Uplink Schemes Based on Space-Time Block Codes and V-BLAST

Mohammed El-Hajjar[†], Salam Zummo[‡], and Lajos Hanzo[†]

[†] School of ECS, University of Southampton, UK.
Email: {meh05r,lh}@ecs.soton.ac.uk

Outline

- ❏ Overview of the State-of-the-art
- ❏ Cooperation Strategies
- ❏ Adaptive System 1
- ❏ Adaptive System 2
- ❏ Conclusions and Future Work

Key References

- L. Hanzo, C. Wong, and M. Yee, *Adaptive wireless transceivers: turbo-coded, turbo-equalized and space-time coded TDMA, CDMA, and OFDM systems.* Chichester, UK: John Wiley and Sons, 2002.
- A. Sendonaris, E. Erkip, and B. Aazhang, "User cooperation diversity. Part I. System description," IEEE Transactions on Communications, 2003.
- G. Scutari and S. Barbarossa, "Distributed space-time coding for regenerative relay networks," IEEE Transactions on Wireless Communications, 2005.
- M. Dohler, E. Lefranc, and H. Aghvami, "Space-time block codes for virtual antenna arrays," IEEE International Symposium on Personal, Indoor and Mobile Radio Communications, 2002.
- E. C. Van Der Meulen, "Three-terminal communication channels," Adv. Appl. Prob. 3, 1971.
- T. Cover, A. El Gamal, "Capacity Theorems for Relay Channel," IEEE Transactions on Information Theory, 1979.
- A. Nosratinia, T. Hunter, A. Hedayat, "Cooperative Communication in Wireless Networks", IEEE Communications Magazine, 2004.
- N. Ahmed, M. A. Khojastepour, B. Aazhang, "Outage Minimization and Optimal Power Control for the Fading Relay Channel", IEEE Information Theory Workshop, 2004.
- J.N. Laneman, D. Tse, G. Wornell, "Cooperative Diversity in Wireless Networks: Efficient Protocols and Outage Behaviour," IEEE Transactions on Information Theory, 2004.

Multiple Input Multiple Output Systems

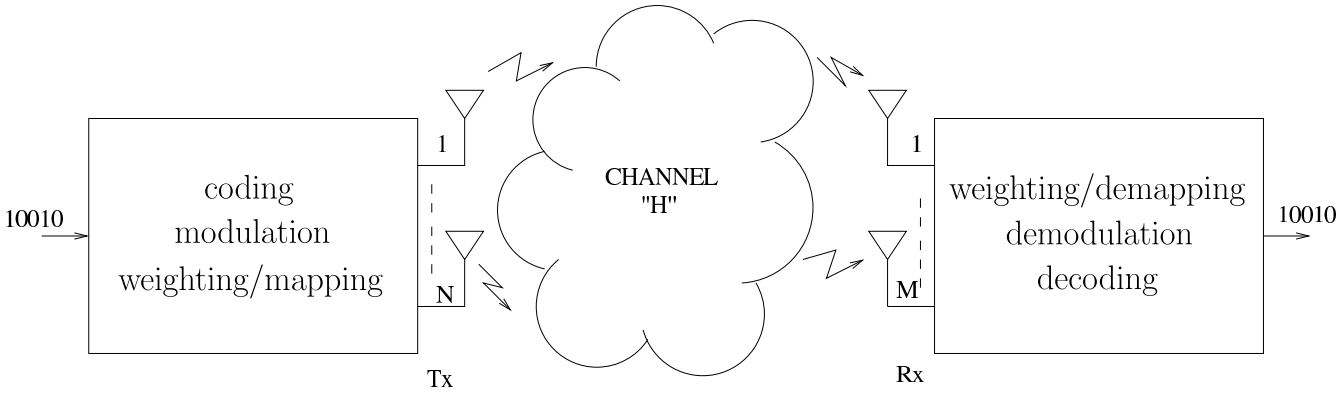

- Benefits?

  Increase of capacity by a factor of min{M,N}

- How?

  Mitigating multipath fading

- Challenges

  Channel estimation, synchronization, power control, resource-allocation/relay-selection, multiplexing loss.

Cooperation in Wireless Networks

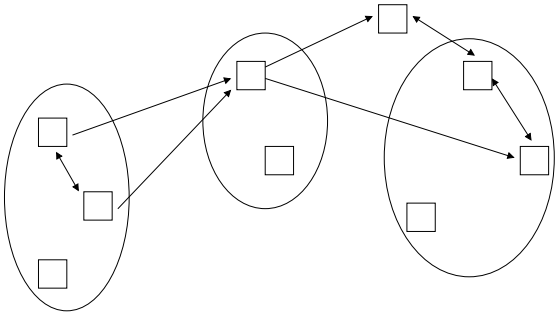

- Transmit diversity requires more than one antennas at the transmitter.
- However, many wireless devices are limited by size, cost and hardware complexity.
- By using cooperative communications, several transmitters or receivers may share their antennas to form a virtual or distributed multiple-antenna system.
- Distributed nodes re-transmit the signal either in a regenerative or non-regenerative fashion.

Cooperation Strategies

- Virtual MIMO
  - Transmitting nodes have to dedicate resources to exchange their data. What is the optimum split of:
    - primary versus secondary signalling
    - When also considering the detrimental effects of extra interference.
  - Use space-time code for transmission.

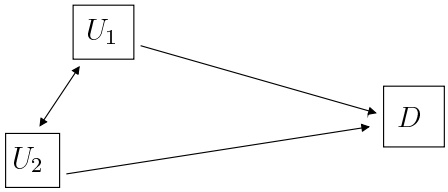

- Relaying
  1. Decode-and-Forward
  2. Compress-and-Forward
  3. Amplify-and-Forward

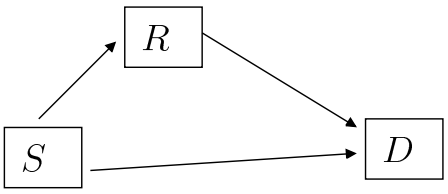

Nodes can use orthogonal or non-orthogonal channels.

Relay Operation

- Full Duplex

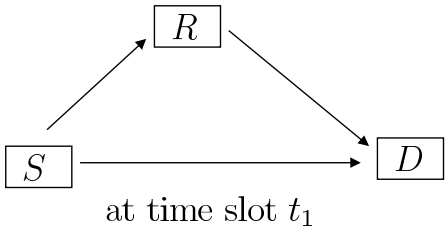

- Half Duplex (simultaneous transmission and reception is unrealsitic)

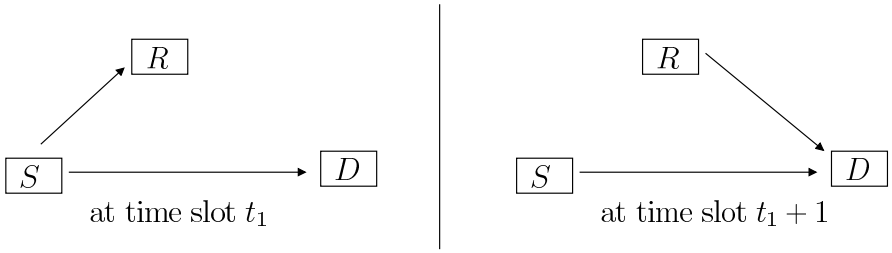

Virtual MIMO

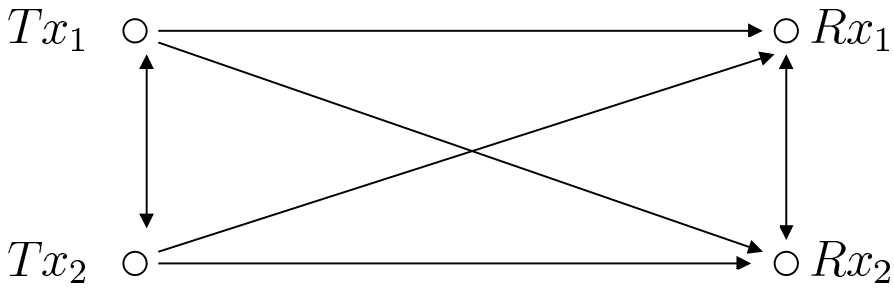

- Tx_1 and Tx_2 exchange data for cooperation (virtual STC or SDM).
- Tx_1 and Tx_2 broadcast data.
- Tx_1 and Tx_2 cooperation as well as Rx_1 and Rx_2 cooperation form a virtual MIMO system.

❑ Use antennas for diversity

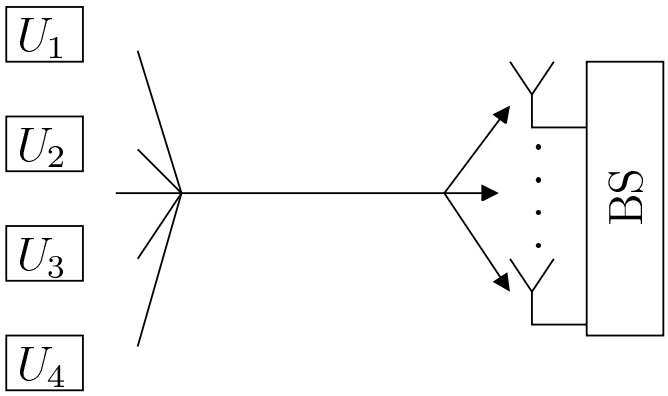

❑ Use antennas for multiplexing

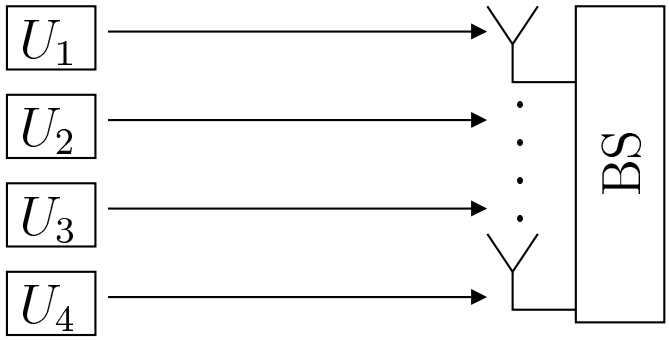

System 1

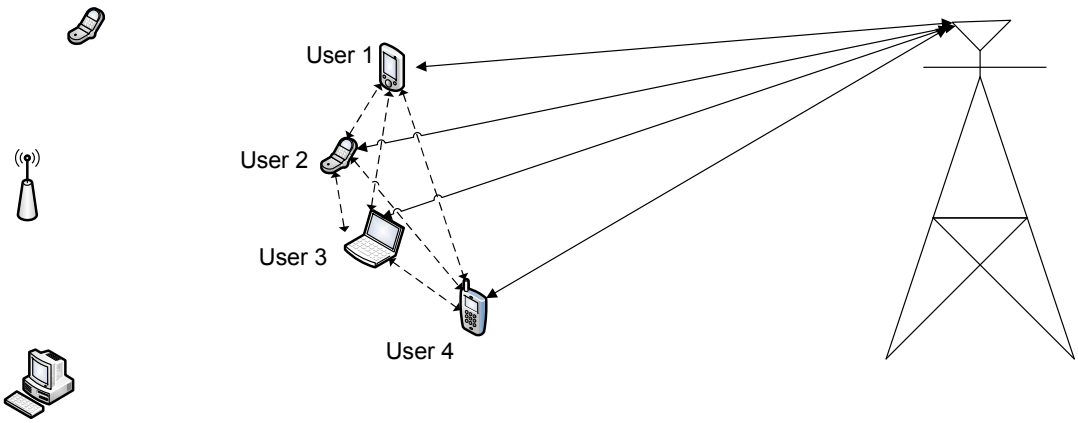

System 1 Exploit users' or MSs'antennas for diversity.

- ❏ MS 1 broadcasts its data in time slot 1.
- ❏ MS 2 broadcasts its data in time slot 2.
- ❏ MS 3 broadcasts its data in time slot 3.
- ❏ MS 4 broadcasts its data in time slot 4.
- ❏ Four users transmit in a G4-like STBC configuration.
- ❏ total number of time slots for transmission is 12.
- ❏ Can save one time slot if the BS can receive the users' data while the cooperating users are exchanging their data.

- ❏ In order to increase the bandwidth efficiency of the system, Adaptive Quadrature Amplitude Modulation (AQAM) can be combined together with the proposed cooperative scheme.
- ❏ The adaptation is carried out according to the following table, while maintaining a target BER of 10^{-3}.

No. of users per cluster	4
No. of Rx Antennas	1
Mode 1	$G4$ STBC, BPSK BE= 0.364 bits/sec/Hz
Mode 2	$G4$ STBC, QPSK BE=0.727 bits/sec/Hz
Mode 3	$G4$ STBC, 16-QAM BE=1.454 bits/sec/Hz
Mode 4	$G4$ STBC, 64-QAM BE=2.18 bits/sec/Hz

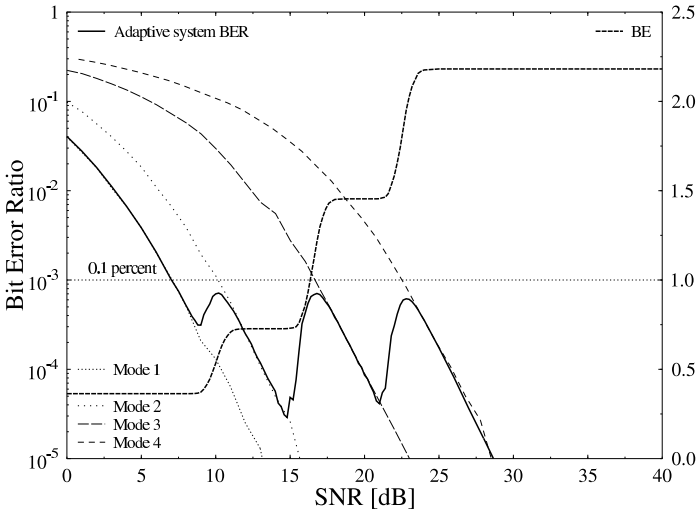

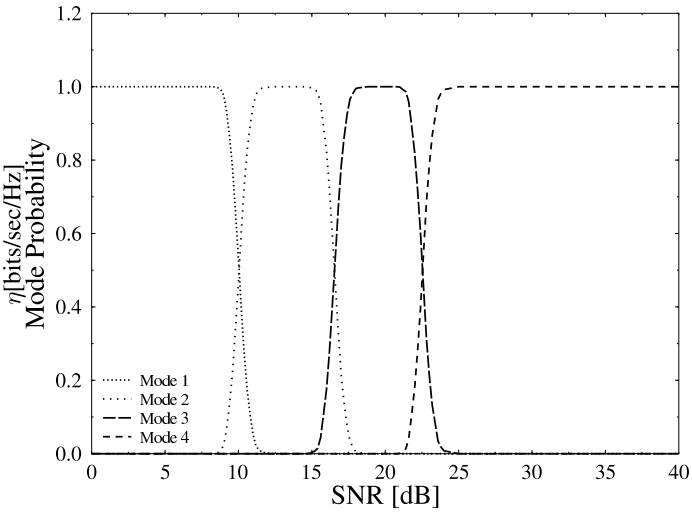

System 1

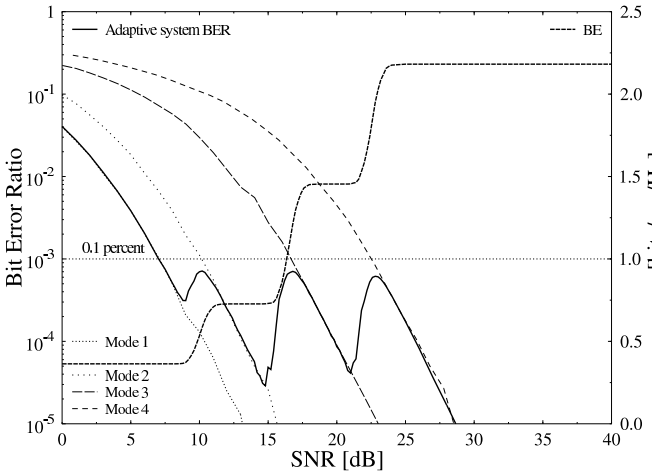

AQAM aided 1Tx, 1Rx non-coop. benchmarker System

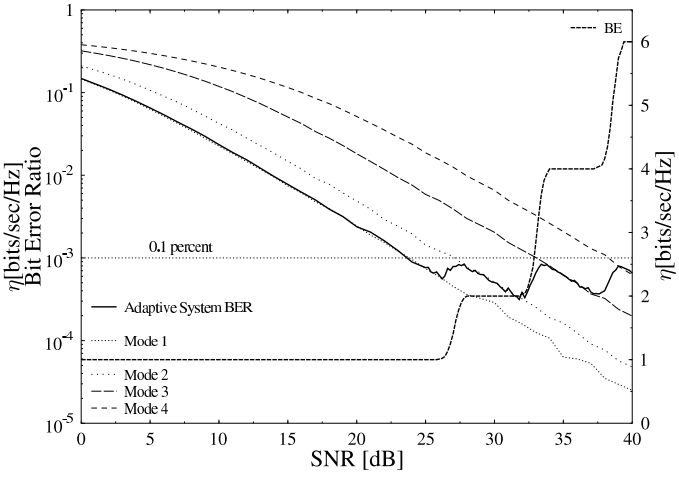

System 1

- ❏ Diversity order of 4.
- ❏ Transmit four users data in 11 time slots.

Benchmarker Scheme

- ❏ Diversity order of 1.
- ❏ Transmit four MSs' data in 4 time slots.

Thus, the proposed Scheme has a higher diversity than a non-cooperative system and hence reaches the target BER at SNR of 7.5 dB as compared to SNR of 23 dB for the non-cooperative system.

This is achieved at the expense of a throughput reduction in the proposed scheme as seen in the figures.

System 2

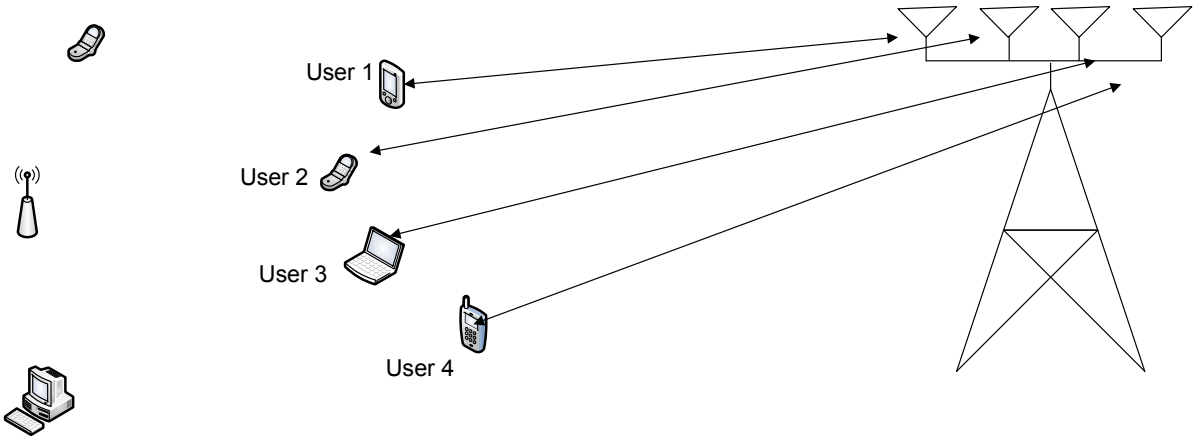

System 2 Exploit the users' or MSs' antennas for Multiplexing.

- ❏ Four users transmit in a four-layer V-BLAST-like transmission configuration.
- ❏ Adaptation is carried out according to the following table; (BE: Bandwidth Efficiency)

No. of users per cluster	4
No. of Rx Antennas	4
Mode 1	one user BE=2 bits/sec/Hz
Mode 2	Two users BE=4 bits/sec/Hz
Mode 3	Three users BE=6 bits/sec/Hz
Mode 4	Four users BE=8 bits/sec/Hz

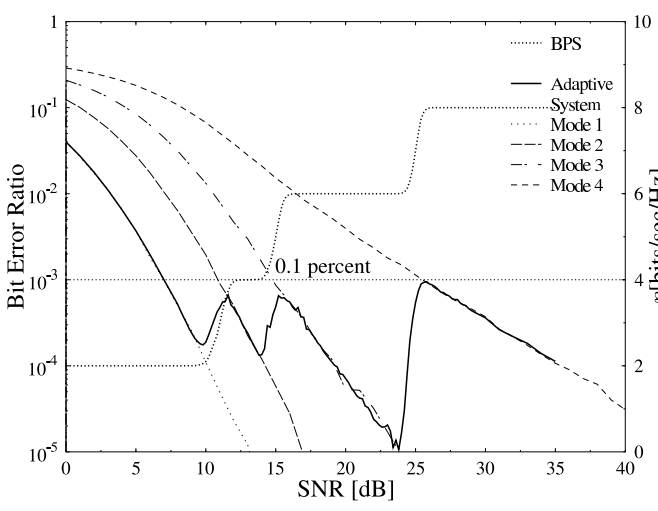

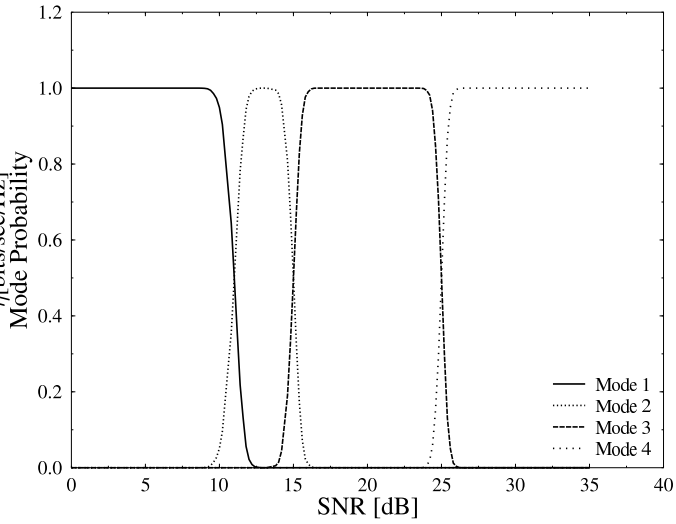

System 2

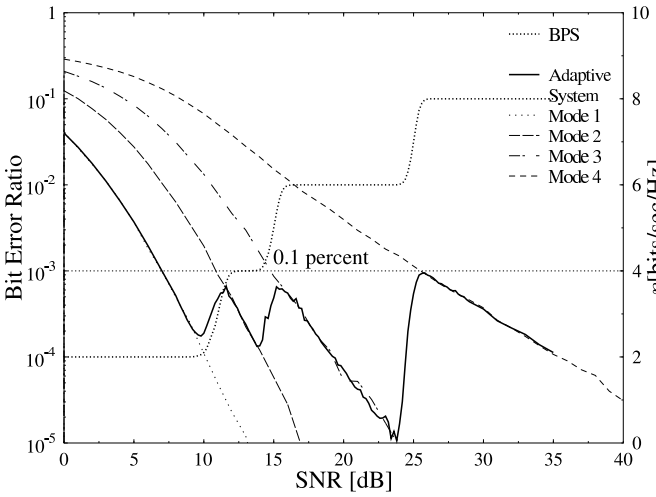

Non-Coop. benchmarker System

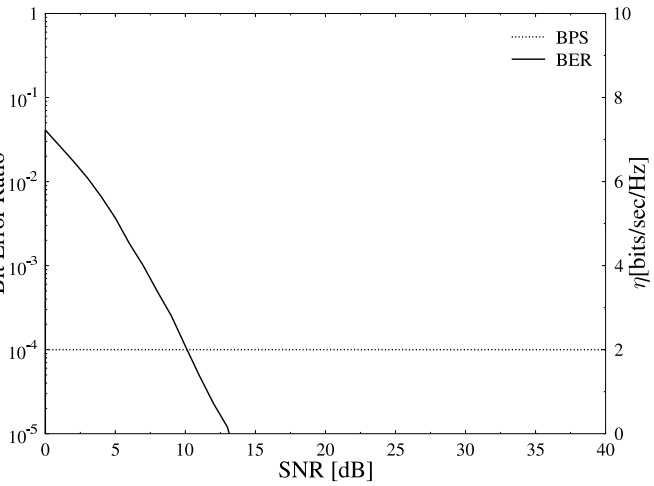

Conclusions

- We proposed two adaptive systems, which amalgamate the advantages of cooperative diversity, distributed STBC as well as V-BLAST, while near-instantaneously adapting the system configuration for the sake of achieving the highest possible throughput, while maintaining a given target BER of 10^{-3}.
- System 1 benefits from a higher diversity gain with the aid of STBC while varying the BE by adapting the modulation scheme employed. System 1 is capable of maintaining a BE between 0.364 bits/sec/Hz and 2.18 bits/sec/Hz.
- System 2 benefits from the higher multiplexing gain of V-BLAST and thus has an effective BE varying between 2 bits/sec/Hz and 8 bits/sec/Hz.

Future Work

- ❏ Mathematical performance analysis of the two proposed systems.
- ❏ Design of an optimised adaptive scheme, where adaptation will be based on the reliable channel quality metric of the estimated BER value of the received frames', rather than on the less reliable channel-SINR metric.

A Detailed Design Example

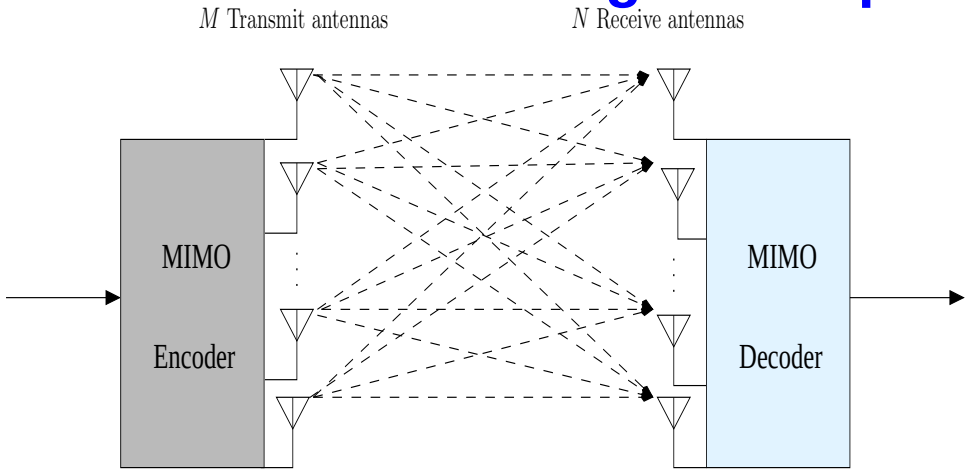

Questions concerning the design of MIMO systems:

- (Q1) How can we achieve the maximum diversity gain, while maintaining a high throughput?
- (Q2) How can we contrive practical near-capacity schemes for arbitrary MIMO configurations for operating right across a wide SNR region, rather than at a single SNR value?

Orthogonal Approach for Diversity-Oriented STBCs

- Alamouti's scheme:

$$\mathbf{G}_2 = \begin{pmatrix} s_1 & s_2 \\ -s_2^* & s_1^* \end{pmatrix}.$$

- $\mathbf{G}_2$ is an orthogonal/unitary matrix.

- Simple single-symbol decoding.

- Orthogonality can be relaxed to create Quasi-Orthogonal STBCs (QO-STBCs).

- Can we view $\mathbf{G}_2$ differently?

Layered Approach

- The Alamouti scheme:

$$\mathbf{G}_2 = \begin{pmatrix} \boxed{s}_1 & s_2 \\ -s_2^* & \boxed{s}_1^* \end{pmatrix}.$$

- Two layers, each layer encoded using repetition coding.

- Orthogonality enables the separation of the layers.

- How many layers can a STBC codeword accommodate?

- How to design better encoding method within each layer?

Linear Dispersion Codes

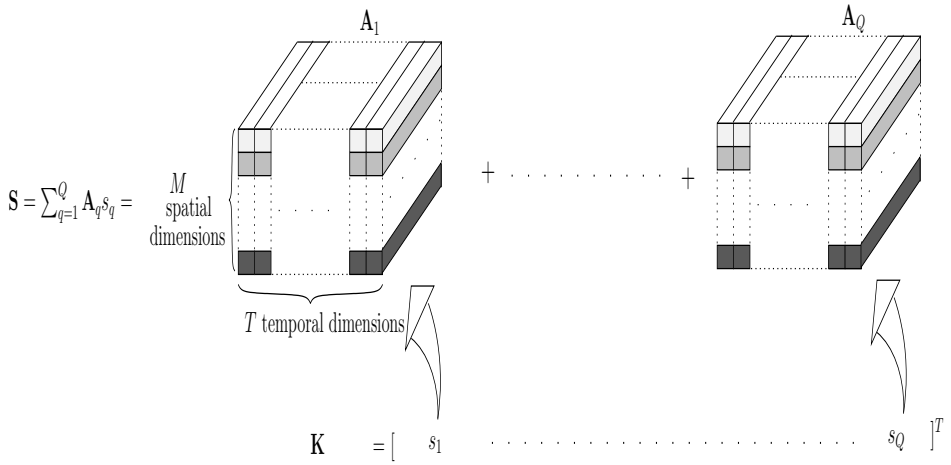

- LDC$(MNTQ)$, with arbitrary modulation schemes.
- Q non-separable layers.
- Optimization of χ.
- A single Dispersion Character Matrix (DCM) χ.

The Burden of Channel Estimation

- Complexity and power consumption.
- Channel estimation errors degrade the attainable performance.

Hence, two questions are asked.

1. How to dispense with the pilot-based channel estimation?
2. At the same time, maintain the general framework of LDCs?

Unified Framework of DLDCs

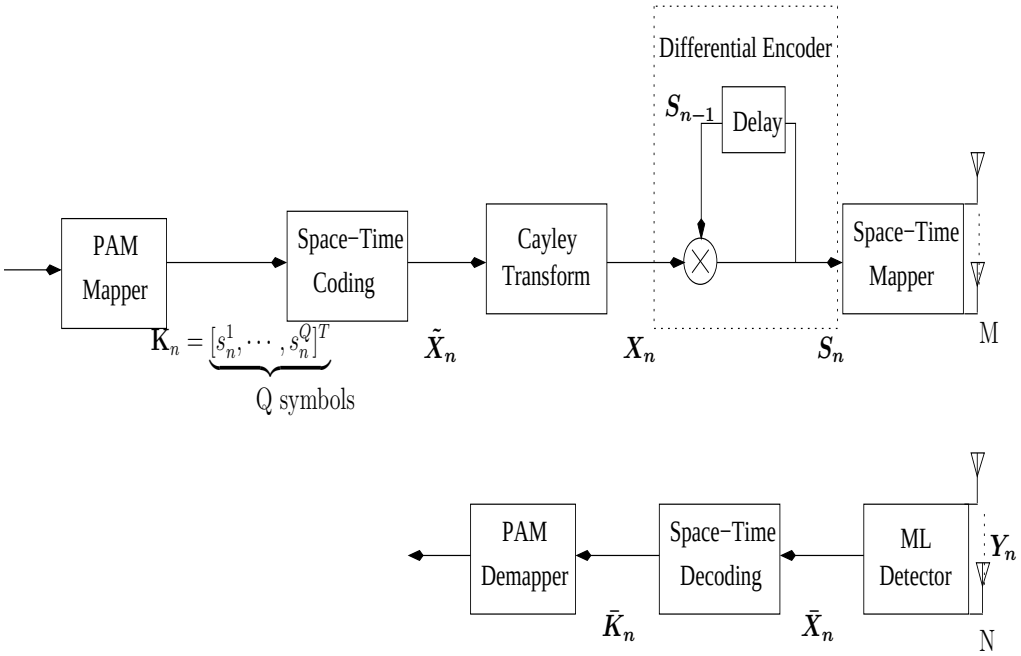

- Differential encoder: $\mathbf{S}_n = \mathbf{S}_{n-1} \cdot \mathbf{X}_n$ imposes the unitary constraint.
- Linear structure: $\tilde{\mathbf{X}}_n = \sum_{q=1}^{Q} \mathbf{A}_q s_q$.
- The Cayley transform: unique mapping between $\tilde{\mathbf{X}}_n$ and $\mathbf{X}_n$.

Cooperative STBCs

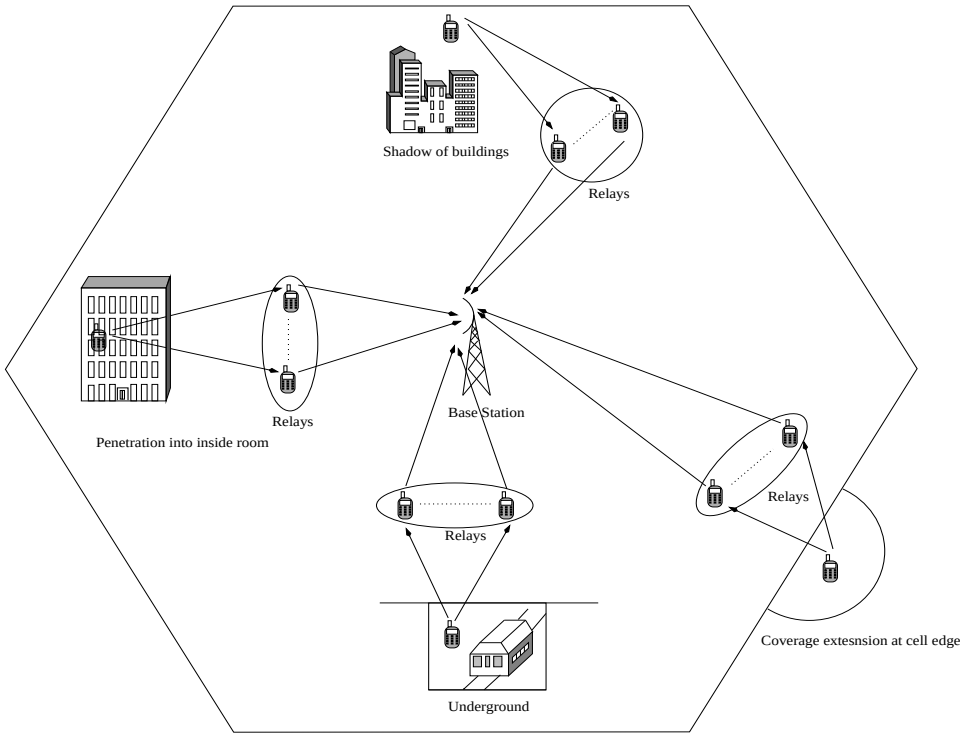

- In cellular networks.
- In wireless sensor networks, ad-hoc networks.

Schematic of the CLDCs

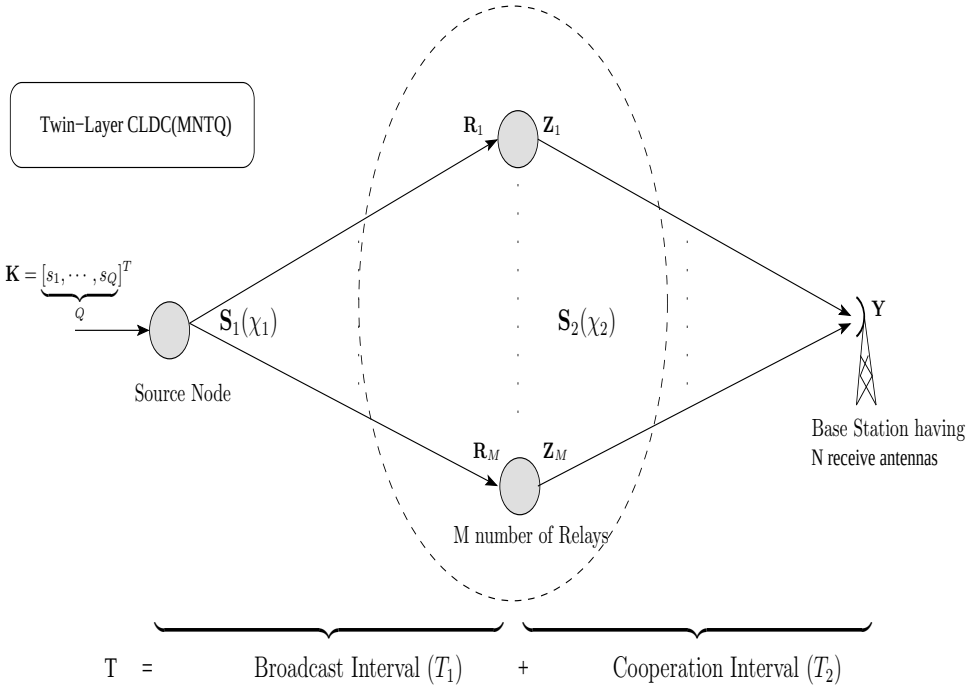

- Two phases of transmission.
- Parameter$(MNTQ)$, $T = T_1 + T_2$.
- How to design $\mathbf{S}_1$ and $\mathbf{S}_2$?

Dispersion Matrices of CLDCs

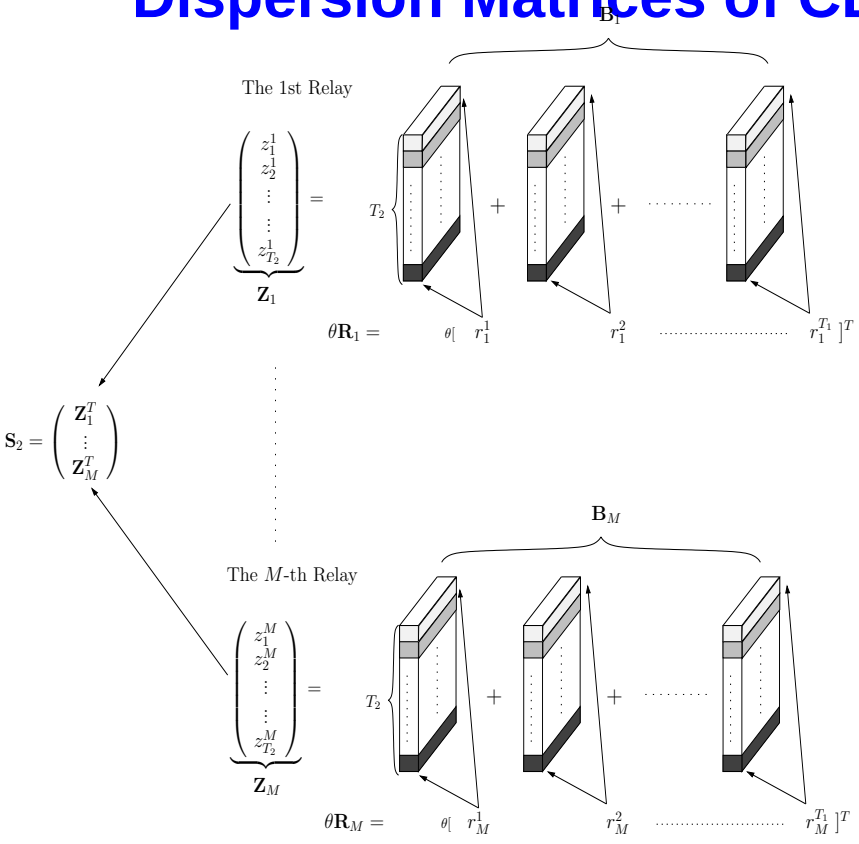

Linking LDCs, DLDCs and CLDCs

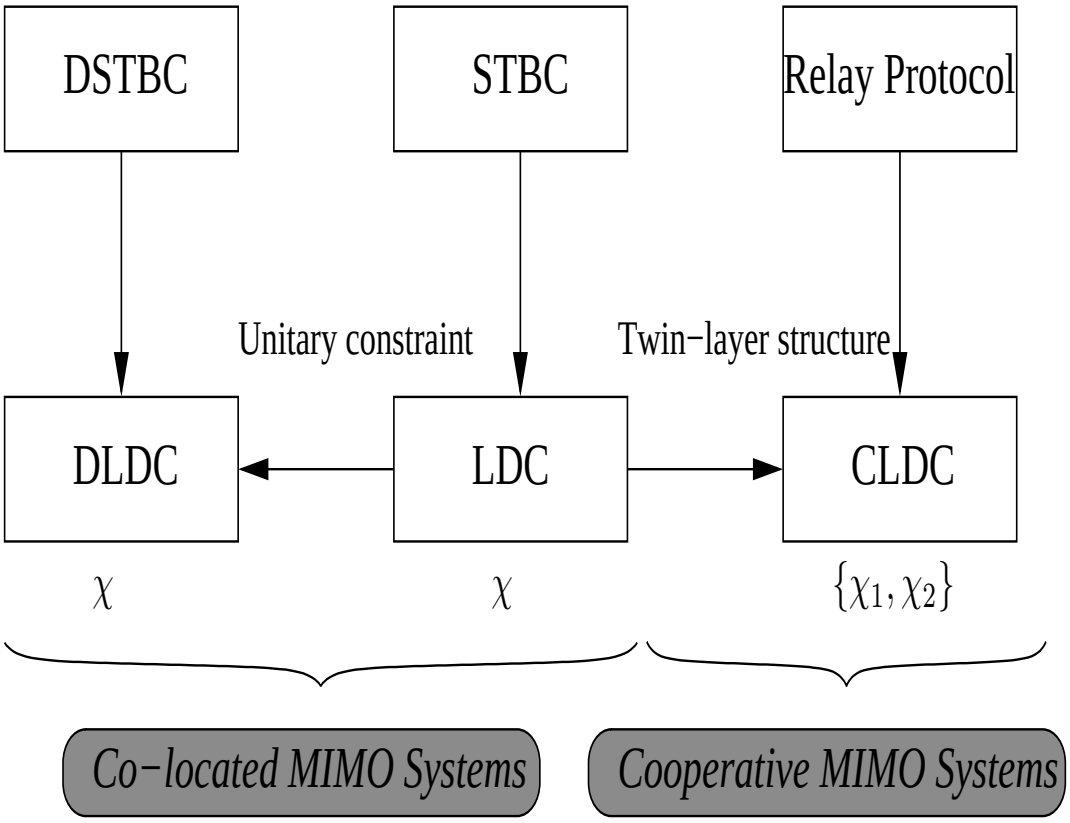

Existing Knowledge

- MIMO channel's capacity.
- Serial Concatenated Codes (SCCs), which are capable of achieving an infinitesimally low BER.
- SCCs can be analyzed and designed using EXIT charts.
- Irregular design principle, using Irregular Convolutional Codes (IRCCs).
- Improving the flexibility using irregular inner codes.

Schematic of the Irregular Scheme

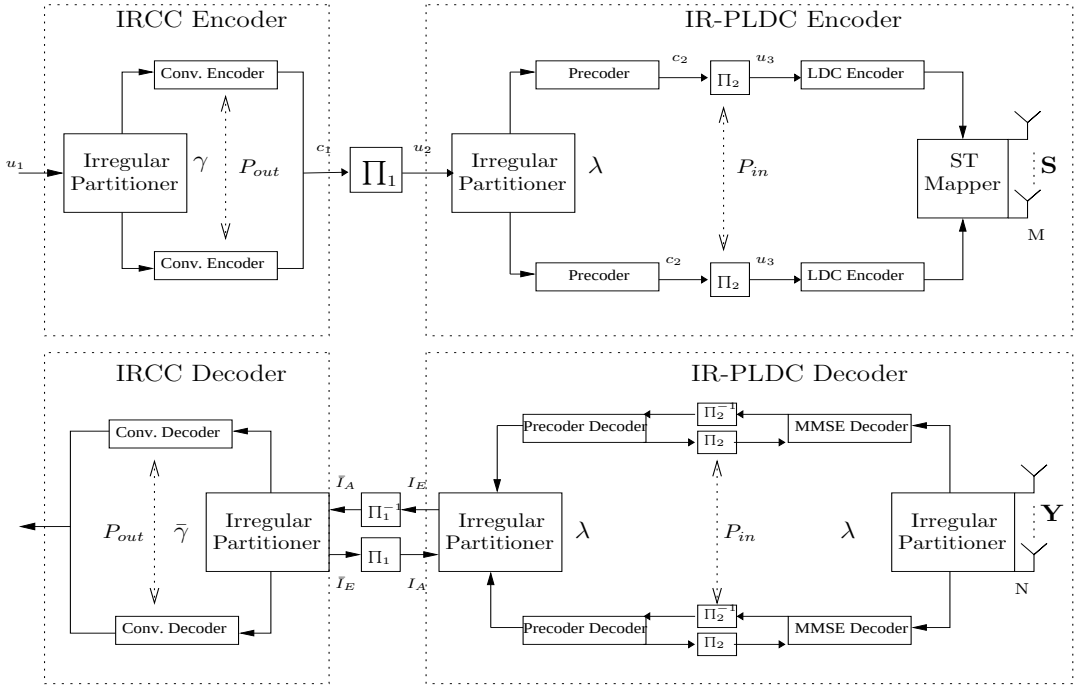

Operational SNR Region

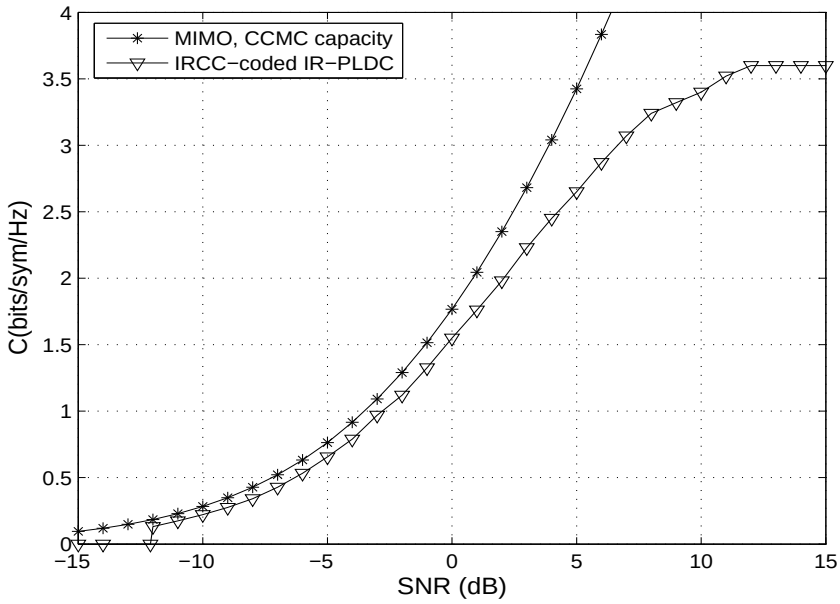

- P_{in} and $P_{out} = 6$.
- The recorded throughput values were achieved by changing γ_{out} and λ_{in}.
- Operational SNR region can be extended.

Small-Scale Fading with *Perfect* CSI

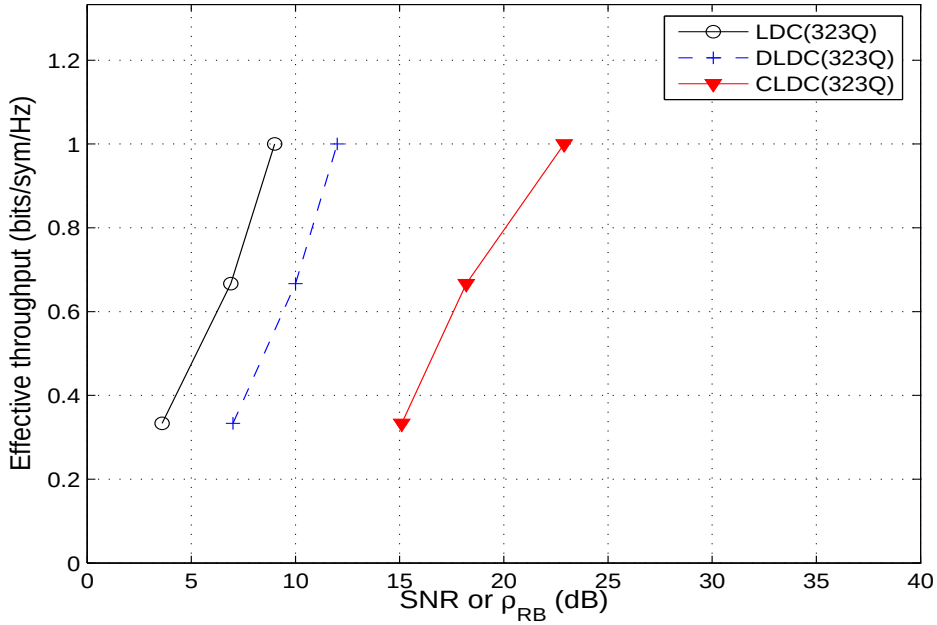

Throughput comparison for the LDCs, the DLDCs and the CLDCs recorded at BER=10^{-4}.

Small-Scale Fading with *Imperfect* CSI

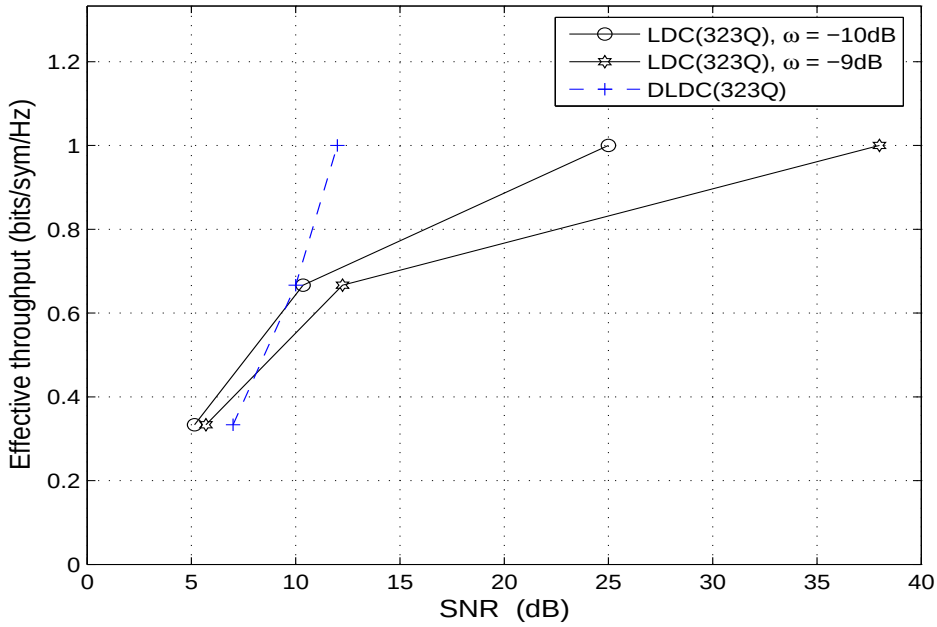

Throughput comparison for the LDCs, the DLDCs and the CLDCs recorded at BER=10^{-4} and the *imperfect* CSI governed by ω (dB).

Large-Scale Shadowing with *Perfect* CSI

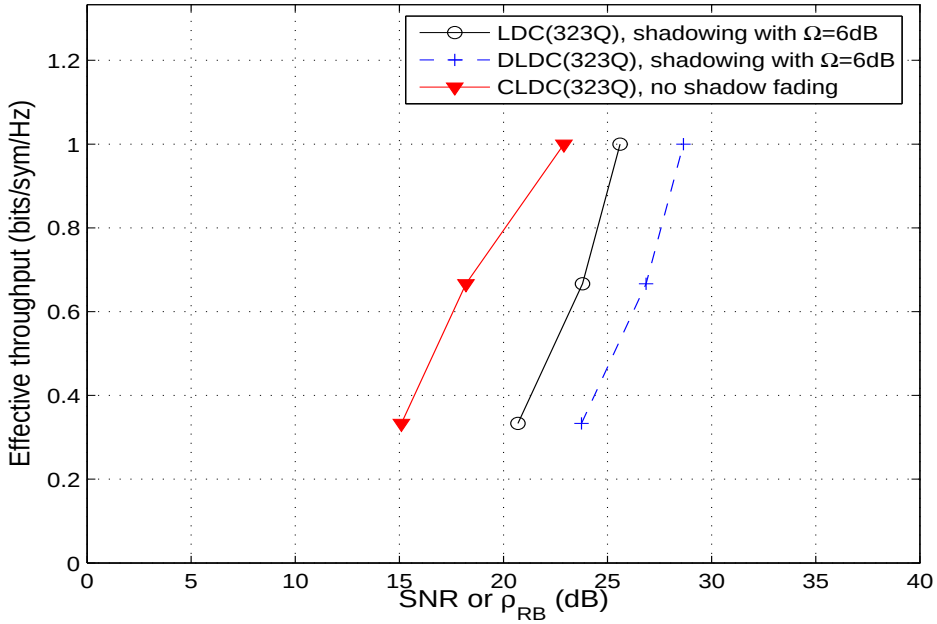

Throughput comparison for the LDCs, the DLDCs and the CLDCs recorded at BER=10^{-4}.

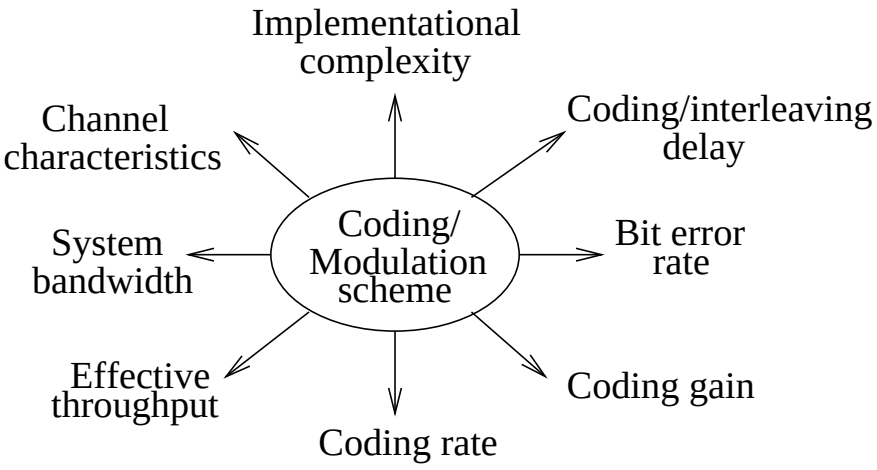

Figure 5: Factors affecting the design of MIMO-aided wireless communications schemes ©John Wiley, Hanzo, Liew, Yeap: Turbo coding, turbo equalization and space-time coding, Wiley & IEEE Press 2002

IEEE Vehicular Technology Conference 2009 Fall

Anchorage

Multiple-Symbol Differential Sphere Detection for the Amplify-and-Forward Cooperative Uplink

Li Wang and Lajos Hanzo

School of Electronics and Computer Science ,

University of Southampton, UK.

Email: lh@ecs.soton.ac.uk

http://www-mobile.ecs.soton.ac.uk

Outline

- ❏ Motivation & Contributions
- ❏ The principle of Multiple-Symbol Differential Sphere Detection (MSDSD)
- ❏ MSDSD Designed for the Amplify-and-Forward Cooperative Uplink
- ❏ Results and Discussions
- ❏ Conclusions

Motivation

- Background
  - It is widely recognized that the Differential Amplify-and-Forward (DAF) transmission scheme is capable of providing a superior performance compared to classic direct transmissions employing differential detection in slow-fading channels.
  - In reality the channels connecting the multiple nodes of a cooperative system typically become time-selective due to the relative mobility of the cooperating terminals.
- Problem To Be Solved:
  - The performance gain achieved by the DAF-aided cooperative system may erode as the environment becomes more time-selective.
  - How to mitigate the performance degradation induced by the relative mobility of the cooperating terminals?

Contributions

- Based on the principle of the single-path Maximum-Likelihood Multiple-Symbol Differential Detection (ML-MSDD) contrived for conventional direct transmission systems, a multi-path ML-MSDD scheme was specifically designed for mitigating the error floor encountered by the DAF-aided user-cooperation assisted system in time-selective channels.
- Sphere Detection (SD) is employed to reduce the complexity imposed by the ML-MSDD, resulting in Mutliple-Symbol Differential Sphere Detection (MSDSD), which is invoked for our DAF-aided cooperative system.

Classification of the Differential Detection

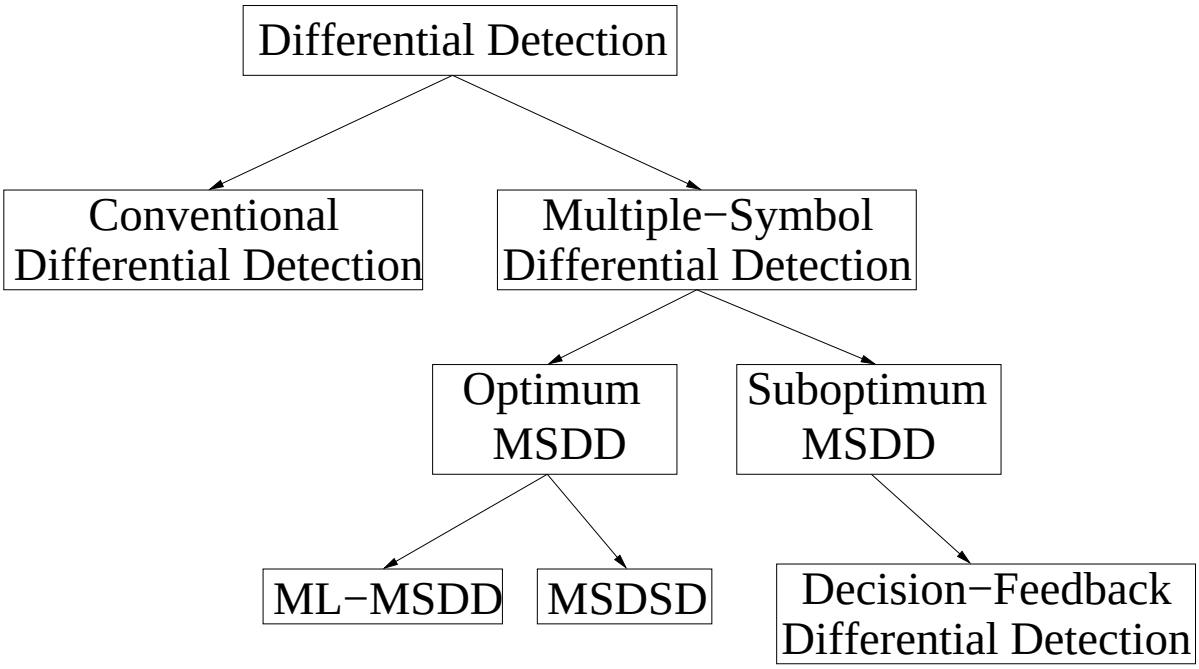

Effects of Doppler Frequency on Conventional Differential Detection (CDD)

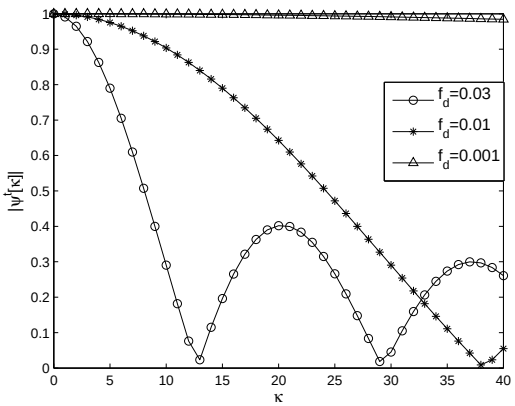

(a) Magnitude of temporal correlation function of Rayleigh fading channels

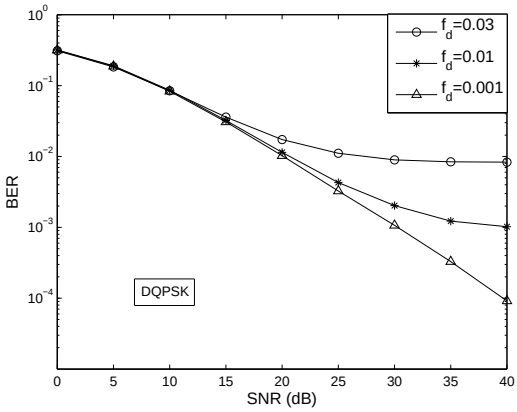

(b) BER of CDD

- The Rayleigh channel's temporal autocorrelation function $\mathcal{E}\{h_k h^*_{k+\kappa}\} = 2\sigma^2 J_0(2\pi B_d T \kappa)$.
- 3dB loss in comparison to the coherent detection aided systems in a slow-fading scenario.
- Time-variant channel (fast fading) significantly degrades the CDD's performance, since the observation window size is only $N_{wind} = 2$.

Principle of the ML-MSDD for Direct Transmission

- *Basic Ideas*:
  - In simple terms, the MSDD is a detector that makes a decision about a block of $(N_{wind}-1)$ consecutive PSK symbols based on N_{wind} received samples.
  - This enables the detector to exploit the correlation between the phase distortions experienced by the consecutive transmitted PSK symbols.
- *ML Metric*:

$$\begin{aligned}\check{\mathbf{s}}_{ML} &= \arg\max_{\mathbf{s}\in\mathcal{C}^N} P(\mathbf{r}|\mathbf{s}) \\ &= \arg\min_{\mathbf{s}\in\mathcal{C}^N} \frac{\exp(-Tr\{\mathbf{r}^H\Psi^{-1}\mathbf{r}\})}{(\pi^{N_{wind}} det\Psi)} \\ &= \arg\min_{\mathbf{s}\in\mathcal{C}^N} Tr\{\mathbf{r}^H\Psi^{-1}\mathbf{r}\},\end{aligned}$$

where the vectors $\mathbf{s}$ and $\mathbf{r}$ contain the consecutively transmitted and received symbols, respectively, and $\Psi = \mathcal{E}\{\mathbf{r}\mathbf{r}^H|\mathbf{s}\}$.

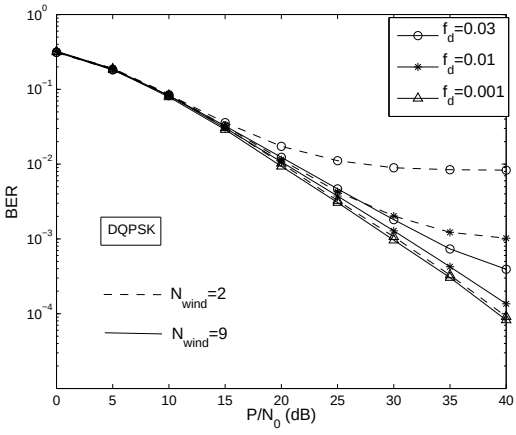

Performance Improved by the ML-MSDD.

Single-Symbol System Model for the DAF-Aided Cooperative System

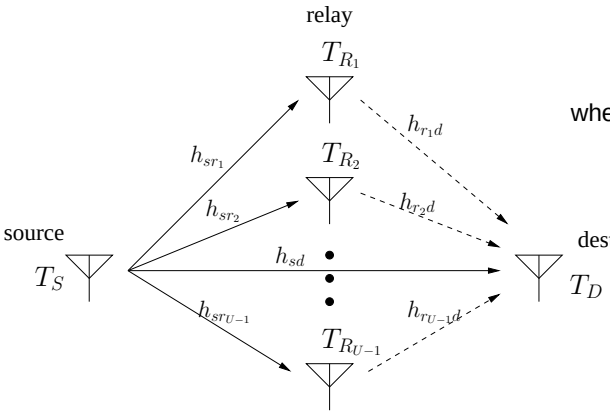

TDMA-Based User-Cooperation Aided System.

- Frame length: L_f.
- Power Constraint: $\sum_{u=1}^{U-1} P_{r_u} = 1 - P_s$, where P_s and P_{r_u} represent the power transmitted by the source node and the uth relay node, respectively.
- The gain factor employed by the uth relay node $f_{AM r_u} = \sqrt{\frac{P_{r_u}}{P_s\sigma^2_{sr_u}+N_0}}$

$$\mathbf{Y}_n = \mathbf{S}_n\mathbf{H}_n + \mathbf{W}_n, \tag{1}$$

where $\mathbf{S}_n$, $\mathbf{H}_n$ and $\mathbf{W}_n$, respectively, are given as follows:

$$\mathbf{S}_n = \text{diag}\{\underbrace{s_{sd}[n],\cdots,s_{sd}[n]}_{U\ elements}\} = \text{diag}\{\underbrace{e^{j2\pi m/M},\cdots,e^{j2\pi m/M}}_{U\ elements}\},$$

$$\begin{aligned}\mathbf{H}_n = \Big[&\sqrt{P_S}h_{sd}[n],\ \sqrt{P_S}f_{AM r_1}h_{sr_1}[n]h_{r_1d}[n+1\cdot L_f], \\ &\cdots,\sqrt{P_S}f_{AM r_{U-1}}h_{sr_{U-1}}[n]h_{r_{U-1}d}[n+(U-1)\cdot L_f]\Big]^T,\end{aligned} \tag{2}$$

$$\begin{aligned}\mathbf{W}_n = \Big[&w_{sd}[n],\ f_{AM r_1}w_{sr_1}[n]h_{r_1d}[n+1\cdot L_f] \\ &+ w_{r_1d}[n+1\cdot L_f],\cdots,f_{AM r_{U-1}}w_{sr_{U-1}}[n]h_{r_{U-1}d} \\ &\times[n+(U-1)\cdot L_f]+w_{r_{U-1}d}[n+(U-1)\cdot L_f]\Big]^T,\end{aligned} \tag{3}$$

Multiple-Symbol System Model for the DAF-Aided Cooperative System

• Then, based on the single-symbol model of Eq. (1), we can construct the *equivalent multiple-symbol system model* as:

$$\underline{\mathbf{Y}} = \underline{\mathbf{S}_d}\underline{\mathbf{H}} + \underline{\mathbf{W}}, \tag{4}$$

where the block matrix $\underline{\mathbf{Y}}$ of the received signal contains N_{wind} user-cooperation based received symbols corresponding to N_{wind} consecutively transmitted differentially encoded symbols $s_{sd}[n], (n = 0, 1, \cdots, N_{wind} - 1)$ of the source node.

• Explicitly: $\underline{\mathbf{Y}} = [\mathbf{Y}_n^T \ \mathbf{Y}_{n+1}^T \ \cdots \ \mathbf{Y}_{n+N_{wind}-1}^T]^T$, and the channel's block matrix $\underline{\mathbf{H}}$ as well as the AWGN block matrix $\underline{\mathbf{W}}$ are defined likewise as $\underline{\mathbf{H}} = [\mathbf{H}_n^T \ \mathbf{H}_{n+1}^T \ \cdots \ \mathbf{H}_{n+N_{wind}-1}^T]^T$, and $\underline{\mathbf{W}} = [\mathbf{W}_n^T \ \mathbf{W}_{n+1}^T \ \cdots \ \mathbf{W}_{n+N_{wind}-1}^T]^T$, respectively.

• Moreover, the diagonal block matrix of the transmitted signal is constructed as $\underline{\mathbf{S}_d} = diag\{\mathbf{S}_n, \ \mathbf{S}_{n+1}, \ \cdots, \ \mathbf{S}_{n+N_{wind}-1}\}$.

ML Metric for the MSDSD Designed for the DAF-Aided Cooperative System

❑ *ML-MSDD Metric*: Based on the multiple-symbol system model of Eq. (4), the decision metric of the ML-MSDD can be expressed as:

$$\underline{\hat{\mathbf{S}}_{ML}} = \arg \min_{\underline{\mathbf{S}} \in \mathcal{C}^{N_{wind}}} Tr\{\underline{\mathbf{Y}}^H \underline{\Psi}^{-1} \underline{\mathbf{Y}}\}, \tag{5}$$

where the conditional autocorrelation matrix is:

$$\underline{\Psi} = \underline{\mathbf{S}_d}(E\{\underline{\mathbf{H}}\underline{\mathbf{H}}^H\} + \mathcal{E}\{\underline{\mathbf{W}}\underline{\mathbf{W}}^H\})\underline{\mathbf{S}_d}^H = \underline{\mathbf{S}_d}\mathbf{C}\underline{\mathbf{S}_d}^H \tag{6}$$

❑ *Transformation to MSDSD Metric*: Then, by further constructing a $(UN_{wind} \times U^2 N_{wind})$-element upper-triangular block matrix $\mathbf{U}$ as:

$$\mathbf{U} \triangleq (\mathbf{F}T_d(\underline{\mathbf{Y}}))^*, \tag{7}$$

where the $(UN_{wind} \times UN_{wind})$-element upper-triangular matrix $\mathbf{F}$, which satisfies $\mathbf{F}^H\mathbf{F} = \mathbf{C}^{-1}$ with the aid of Cholesky factorization, we finally arrive at:

$$\underline{\hat{\mathbf{S}}_{ML}} = \arg \min_{\mathbf{s} \leftrightarrow \underline{\mathbf{S}} \in \mathcal{C}^{N_{wind}}} ||\mathbf{U}\mathbf{s}||^2 \leq R, \tag{8}$$

❑ *Tree Search within a Confined Hyper-Sphere*: Since we have an upper-triangular block matrix $\mathbf{U}$, a tree search can be carried out from the $(n = N_{wind} - 1)$th element of $\mathbf{s}$ downwards to the $(n = 1)$th element, making sure that the accumulated Partial Euclidean Distance (PED) does not exceeds the introduced search radius R.

❑ *Search Radius Update*: The search radius R is updated by calculating the Euclidean distance between the newly obtained signal point $\check{\mathbf{s}}$ and the origin. Then a new search is carried out with the updated search radius.

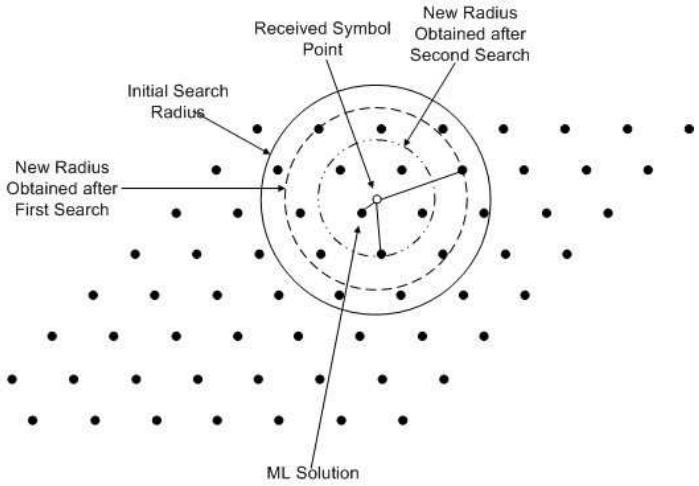

MSDSD Tree Search Example (DBPSK, $N_{wind} = 5$)

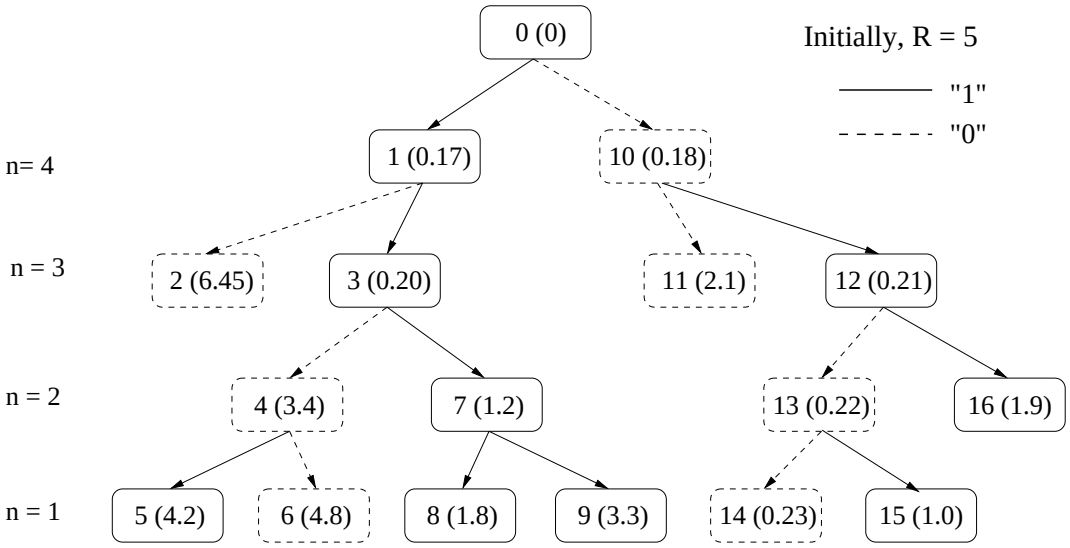

Figure 6: Illustration of the MSDSD algorithm with the aid of the classic tree searching: The figure in ( ) indicates the PED of a specific node for the trial point in the modulated constellation; while the number outside represents the order in which the points are visited.

BER Performance

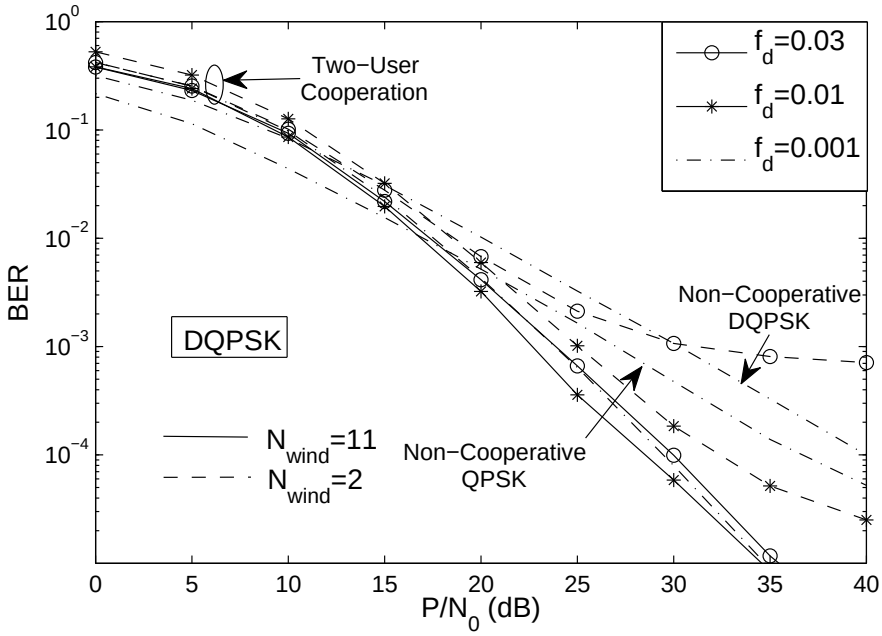

Complexity Reduction Achieved by the MSDSD in Two-User Cooperation Scenarioblack

- A potentially excessive-complexity search is likely to be encountered when ML-MSDD is employed, depending on the size of the constellation M_c and the observation window size N_{wind}, which prevents the application of the full-search-based ML-MSDD detectors in most practical cases.
- For example, in the scenario of using DQPSK ($M_c = 4$) and an observation window size of $N_{wind} = 11$, the number of PED evaluations per symbol block is: $\frac{M_c^{(N_{wind}-1)}}{N_{wind}} = \frac{4^{10}}{11}$.

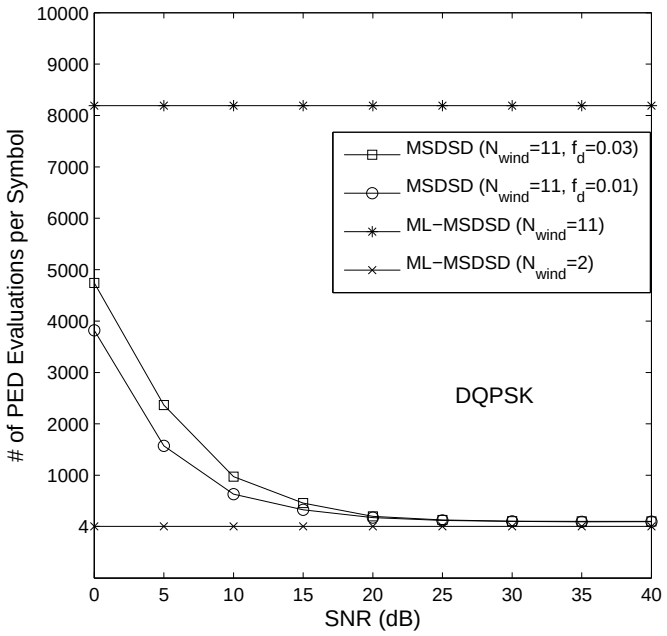

Conclusions

- A MSDSD scheme was proposed for mitigating the error floor encountered by the DAF-aided user-cooperation aided system in time-selective channels, leading to a significant performance gain over the system using the CDD at a relatively low complexity.
- For example, given a target BER of 10^{-3}, a performance gain of about 10 dB can be attained by the proposed MSDSD employing $N_{cand} = 11$ for a DQPSK modulated cooperative two-user system in a relatively fast-fading channel having a normalized Doppler frequency of 0.03.

IEEE Vehicular Technology Conference 2009 Fall
Anchorage, Alaska, USA

Distributed Self-Concatenated Codes for Low-Complexity Power-Efficient Cooperative Communication

M. F. U. Butt, R. A. Riaz, S. X. Ng and L. Hanzo

School of Electronics and Computer Science ,
University of Southampton, UK.
Email: lh@ecs.soton.ac.uk
http://www-mobile.ecs.soton.ac.uk

Outline

- Introduction and Motivation
- SECCC-ID
  - Binary SECCC-ID
  - Non Binary SECCC-ID
- System Model
  - DSECCC-ID Encoder
  - DSECCC-ID Decoder
- Design and Analysis Using EXIT Charts
- Results and Discussions
- Conclusions and Future Research

Key References

- [1] A. Sendonaris, E. Erkip and B. Aazhang, **User cooperation diversity part I: System description,** *IEEE Transactions on Communications*, vol. 51(11), pp. 1927–1938, 2003.
- [2] N. Laneman, D. N. C. Tse and G. W. Wornell, **Cooperative diversity in wireless networks: efficient protocols and outage behavior,** *IEEE Trans. on Information Theory*, vol. 50, no. 12, pp. 3062–3080, 2004.
- [3] M. F. U. Butt, S. X. Ng and L. Hanzo, **EXIT Chart Aided Design of Near-Capacity Self-Concatenated Trellis Coded Modulation Using Iterative Decoding,** in IEEE Vehicular Technology Conference, Marina Bay, Singapore, pp. 734-738, May 2008.
- [4] M. F. U. Butt, R. A. Riaz, S. X. Ng and L. Hanzo, **Near-Capacity Iteratively Decoded Binary Self-Concatenated Code Design Using EXIT Charts,**, *Proceedings of the Global Communications Conference*, Nov/Dec 2008.
- [5] S. ten Brink, **Convergence behavior of iteratively decoded parallel concatenated codes,** *IEEE Transactions on Communications*, vol. 49, pp. 17271737, Oct. 2001.
- [6] B. Zhao and M. C. Valenti, **Distributed turbo coded diversity for relay channel,** *IEE Electronics Letters*, vol. 39, pp. 786–787, May 2003.

Introduction and Motivation

- **Cooperative Diversity Scheme [1,2]**
  - *small mobile unit: correlation of signals in MIMO.*
  - User cooperation: independent fading.
  - *Decode-And-Forward: error propagation.*
  - *Amplify-And-Forward: noise enhancement.*
- **Self-Concatenated Convolutional Codes with Iterative Decoding (SECCC-ID)**
  - Low complexity scheme invoking a single encoder and decoder [3,4].
  - EXIT chart analysis gives insight into decoding convergence behaviour [5].
- **Distributed Turbo Coding Scheme [6]**
  - Power efficient.
  - *Assumming a perfect source-relay link.*

Non-binary SECCC-ID

- An SECCC-ID scheme was designed using Trellis Coded Modulation (TCM) as constituent codes [3].
- The proposed design was symbol-based, therefore it had the inherent problem of exhibiting a mismatch between the EXIT curve and the bit-by-bit decoding trajectory.
- The studies published in the literature of SECCC-ID scheme do not aim for finding good codes in terms of decoding convergence.
- An EXIT chart based analysis of the iterative decoder provides an insight into its decoding convergence behaviour and hence it is helpful for finding the best constituent codes for SECCC-ID without time-consuming bit-by-bit simulation of the actual system.
- The SNR value, where the turbo-cliff in the BER curve of a concatenated code appears can be successfully predicted with the aid of EXIT charts.
- However, the EXIT chart computation assumes the employment of a sufficiently long interleaver, so that the LLRs may be rendered Gaussian distributed.

Non Binary SECCC-ID Analysis Using EXIT charts

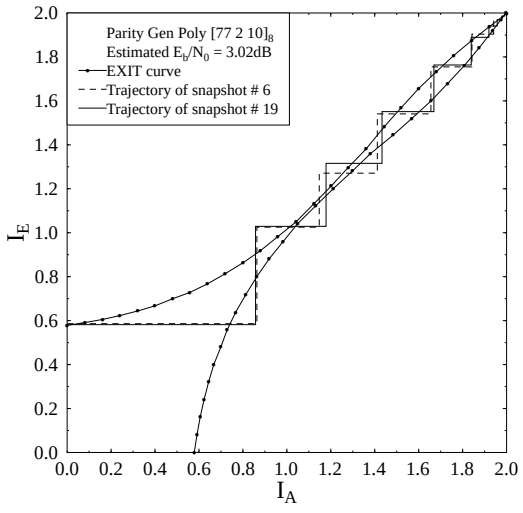

Fig 1. *EXIT chart and two snapshot decoding trajectories for half-rate 4PSK-assisted non binary SECCC-ID using a block length of* 10^4 *symbols at* $E_b/N_0 = 3.02$ *dB.*

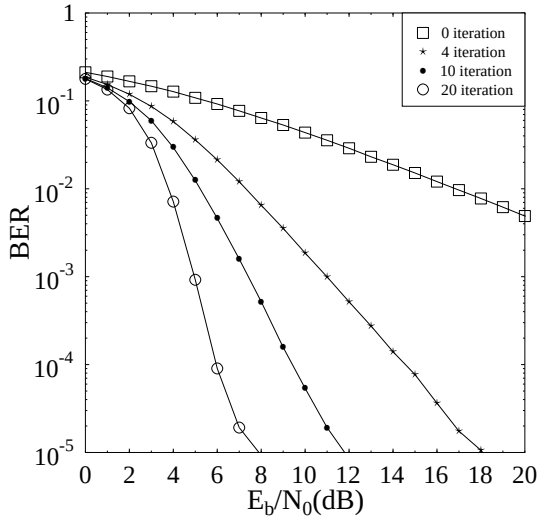

Fig 2. *Simulations results for half-rate non binary SECCC-ID Code when communicating over uncorrelated Rayleigh fading channels.*

Binary SECCC-ID

- The bit-based design eliminates the mismatch inherited by the symbol-based design [4].
- RSC encoder using the generator polynomials G=[13 15]$_8$ with a rate of $R_1 = 1/2$ and memory $\nu = 3$. Then there is an interleaver followed by a rate $R_2 = \frac{3}{4}$ puncturer. The overall code rate becomes $R = \frac{R_1}{2 \times R_2} = \frac{1/2}{2(3/4)} = \frac{1}{3}$.

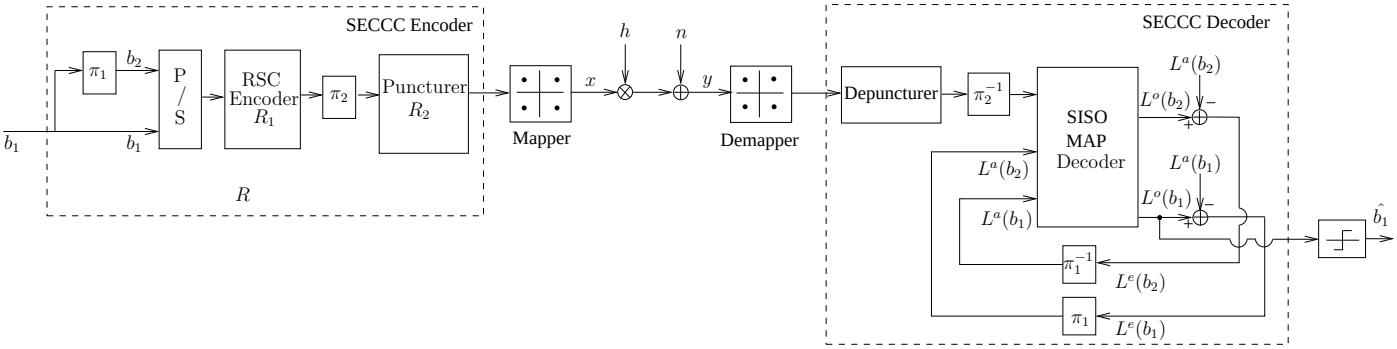

Fig 3. *The block diagram of binary SECCC-ID System.*

Self-concatenated Decoder

- The received signal is passed through a soft demapper to calculate the conditional probability density function (PDF) of receiving y, when $x^{(m)}$ was transmitted:

$$P(y|x^{(m)}) = \frac{1}{\pi N_0} \exp\left(-\frac{\left|y - hx^{(m)}\right|^2}{N_0}\right), \tag{9}$$

  where $x^{(m)}$ is the hypothetically transmitted QPSK symbol for $m \in \{0,1,2,3\}$.
- These probabilities are passed to a soft-value depuncturer, which converts them to bit-based Log-Likelihood Ratios (LLRs) and inserts zero LLRs at the punctured bit positions. These are then deinterleaved and fed to the Soft-Input Soft-Output (SISO) *Maximum A Posteriori Probability* (MAP) decoder.
- The decoder calculates the extrinsic LLR of the information bits, namely $L^e(b_1)$ and $L^e(b_2)$. They are appropriately interleaved to yield the *a priori* LLRs of the information bits, namely $L^a(b_1)$ and $L^a(b_2)$, as shown in Fig. 3.
- Self-concatenated decoding proceeds, for a fixed number of iterations.

- Distributed Binary Self-Concatenated Coding scheme using Iterative Decoding (DSECCC-ID) for cooperative communications is analyzed with the aid of EXIT charts.
- The realistic condition of having an imperfect source-relay communication link is considered.

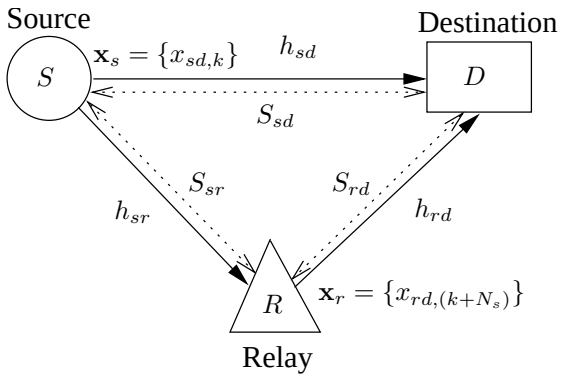

Fig 4. *Schematic of a two-hop relay-aided system.*

- DSECCC-ID Encoder
  - The source node transmits SECCC symbols to both the relay and the destination nodes during the first transmission period.
  - The relay performs SECCC-ID decoding. It then re-encodes the information bits using a Recursive Systematic Convolutional (RSC) code during the second transmission period
  - The resultant symbols transmitted from the source and relay nodes can be viewed as the coded symbols of a three-component parallel-concatenated SECCC-ID encoder.

DSECCC-ID Encoder

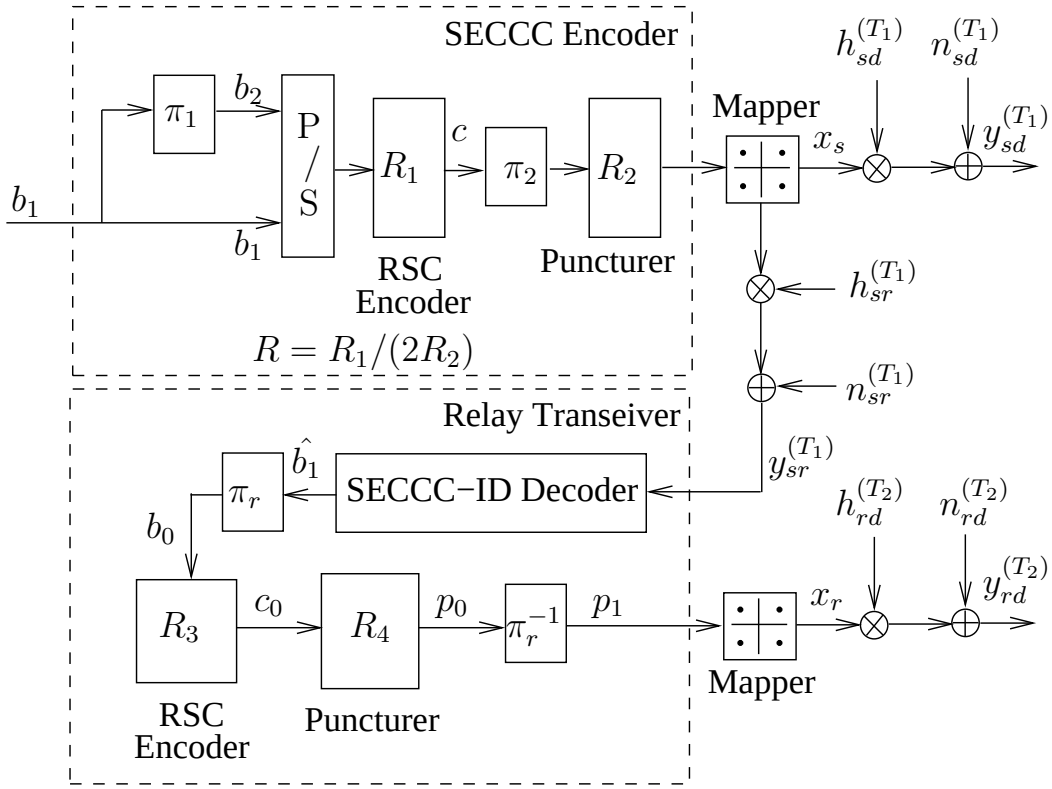

Fig 5. *DSECCC-ID Encoder.*

DSECCC-ID Decoder

- There are two inputs to the RSC MAP decoder block, in Fig. 6.
  - The first is the extrinsic information of bit b_1 provided by the SECCC-ID decoder, which is obtained from the addition of $L^e(b_1)$ and the deinterleaved version of $L^e(b_2)$. The resultant $L_1^e(b_1)$ stream is interleaved by π_r to generate $L^a(b_0)$.
  - The second input of the RSC MAP decoder is the interleaved and depunctured version of the soft information provided by the QPSK demapper denoted as $P(y_{rd}|x_{rd})$.

DSECCC-ID Decoder

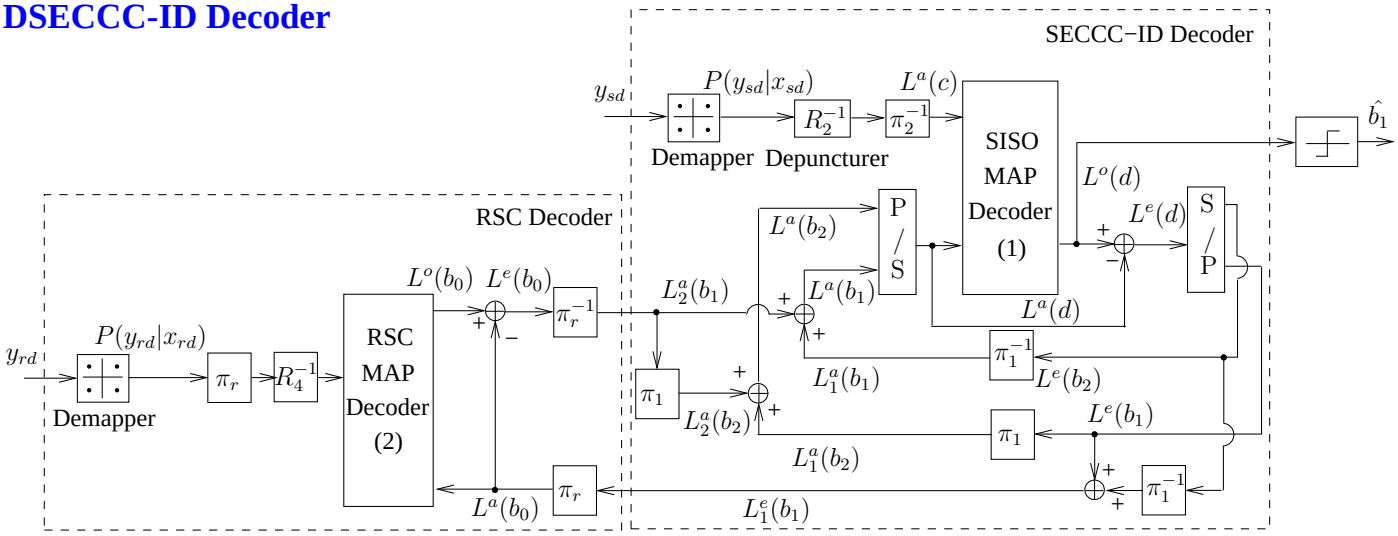

Fig 6. *DSECCC-ID Decoder.*

DSECCC-ID Decoder

- The RSC decoder then provides the improved extrinsic LLR of the data bit b_0 namely $L^e(b_0)$ as its output, which is deinterleaved by π_r^{-1} to yield $L_2^a(b_1)$. The LLR $L_2^a(b_1)$ can be further interleaved using π_1 to generate $L_2^a(b_2)$.
- These *a priori* LLRs output by the RSC can be added to the SECCC-ID decoder's *a priori* LLRs of b_1 and b_2, thus completing the iteration between the RSC and SECCC-ID decoders.

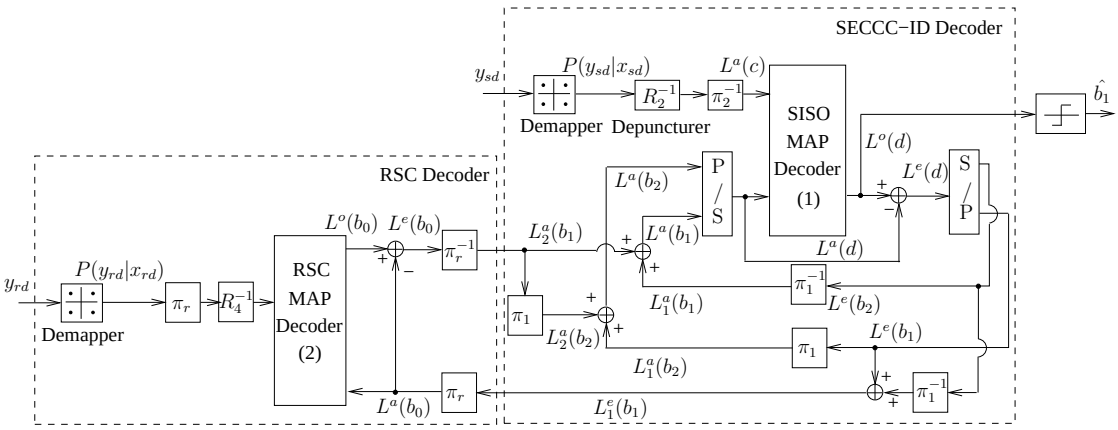

Fig 6. *DSECCC-ID Decoder.*

Binary SECCC-ID Analysis Using EXIT charts

- R_1=1/2 and R_2=3/4, QPSK-assisted SECCC-ID, $\nu = 3$, $\eta = 0.67$ bit/s/Hz achieves decoding convergence at received SNR (SNR_r) = -0.15 dB for transmission over an uncorrelated Rayleigh fading channel.
- Using SNR_r at the relay determine the equivalent SNR at the source node (SNR_e):

$$SNR_r = SNR_e + 10\log_{10}(G_{sr}) \text{ [dB]} \quad (10)$$

- For $G_{sr} = 4$, $SNR_e = -3.5$ dB.

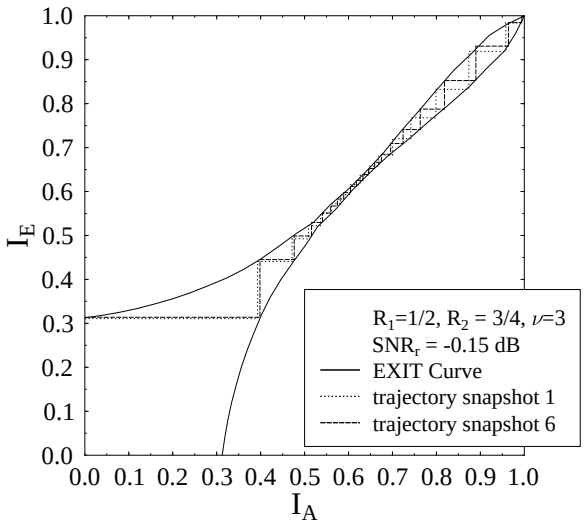

Fig 7. *EXIT chart and 'snap-shot' decoding trajectories of binary SECCC-ID System.*

DSECCC-ID Analysis Using EXIT charts

- Self-concatenated iterations at the source-destination link uses $I_{sd} = 2$ and source-relay link uses $I_{sr} = 8$.
- The number of iterations between the SECCC-ID and RSC at the destination node is $I_{sd,rd} = 12$.
- At the DSECCC-ID decoder we have $I_{DSCC} = I_{sd} \times I_{sd,rd} = 24$ decoding iterations.
- This makes the total decoding iterations in the overall system equal to $I_{sr} + I_{DSCC} = 32$ as compared to a non-cooperative SECCC-ID employing $I = 40$ iterations..

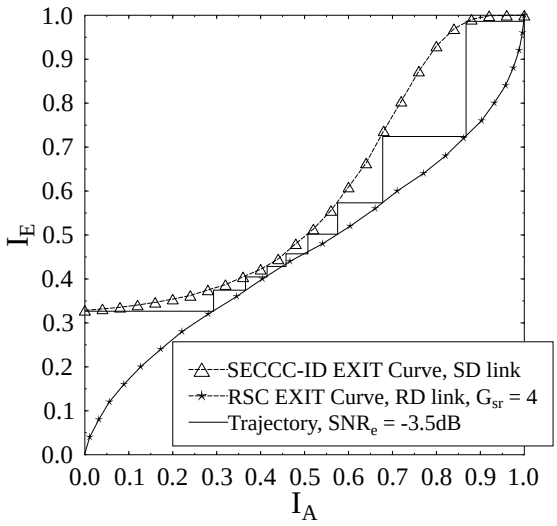

Fig 8. *EXIT charts and a 'snap-shot' decoding trajectory of DSECCC-ID scheme for $SNR_e = -3.5$ dB both at the source as well as at the relay nodes.*

- Our prediction is verified by computing the corresponding Monte-Carlo simulation-related decoding trajectory for the DSECCC-ID scheme for a frame length of 120,000 bits.
- Thus the DSECCC-ID outperforms the SECCC-ID scheme by about 3.35 dB in SNR terms.

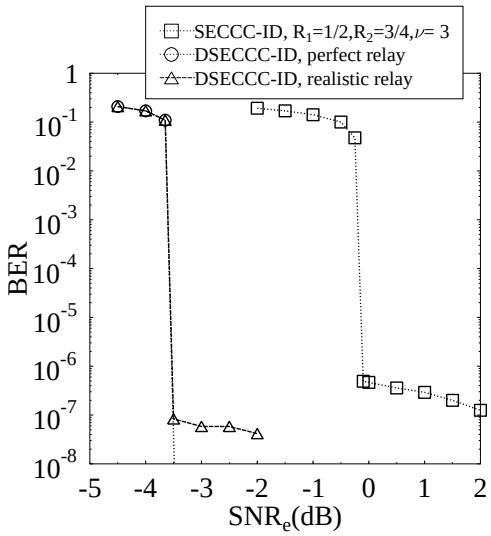

Fig 9. *BER versus SNR_e performance of SECCC-ID and DSECCC-ID schemes.*

Conclusions

- A power and bandwidth efficient DSECCC-ID scheme has been proposed for cooperative communications based on three-component concatenated design.
- To exploit the low complexity offered by SECCC-ID codes we explored their application in distributed cooperative communications.
- Once the received SNR at the relay node exceeds the error-free decoding threshold, the SECCC-ID decoder employed at the relay node becomes capable of reliably decoding the source signals.
- The EXIT chart of the three-component DSECCC-ID decoder seen in Fig. 8 reveals that a beneficial combination of the equivalent SNR of the source and the relay nodes results in a low BER at the destination, despite considering a potentially error-prone reception at the relay.
- Thus we reduced the total power required by the overall system as compared to an SECCC-ID system. The overall complexity of this distributed cooperative communication system is less than a non-cooperative SECCC-ID system.

Future Work

- Near-capacity non-coherently detected DSECCC-ID cooperative schemes.
- Performance for different relay location scenarios and power optimisation in DSECCC-ID.
- Performance Analysis of Hard Versus Soft Relaying in DSECCC-ID.

IEEE ICC'2012
Ottawa, Canada

First-Hop-Quality-Aware Dynamic Resource Allocation for Amplify-and-Forward Opportunistic Relayed SC-FDMA

Jiayi Zhang, Lie-LIang Yang and Lajos Hanzo

Communications Research Group
School of Electronics and Computer Science
University of Southampton, UK.
Email: {lh}@ecs.soton.ac.uk
http://www-mobile.ecs.soton.ac.uk

Key References

- C. Han, **J. Zhang**, L. Hanzo, *et al.*, "Green Radio: Radio Techniques to Enable Energy Efficient Wireless Networks", in *IEEE Commun. Mag. Special Issue: Green Commun.*, vol. 49, no. 6, pp. 46-54, Jun. 2011.
- **J. Zhang**, L.-L. Yang and L. Hanzo, "Energy-Efficient Channel-Dependent Cooperative Relaying for the Multi-User SC-FDMA Uplink", in *IEEE Trans. Veh. Technol.*, vol. 60, no. 3, pp. 992-1004, Mar. 2011.
- W. Dang, M. Tao, *et al.*, "Subcarrier-pair based resource allocation for cooperative multi-relay OFDM systems", in *IEEE ToW*, vol. 9, no. 5, pp. 1640-1649, May 2010.
- Y. Jing, *et al.*, "Single and multiple relay selection schemes and their achievable diversity orders", in *IEEE ToW*, vol. 8, no. 3, pp. 1414-1423, Mar 2009.
- K. B. Letaief, *et al.*, "Dynamic multiuser resource allocation and adaptation for wireless systems", in *IEEE Wireless Commun. Mag.*, vol. 13, no. 4, pp. 38-47, Aug. 2006.
- A. Bletsas, *et al.*, "A simple Cooperative diversity method based on network path selection", in *IEEE J. Sel. Areas Commun.*, vol. 24, no. 3, pp. 659-672, Mar. 2006.

A Cooperative Communication Framework

Why Cooperation?

Aims: improving . . .

Ideal: beneficial multiple-antenna technique – MIMO[a]

Reality: diversity gain is limited by the size of MT

Solution: virtual MIMO – relay-assisted user cooperation, BS cooperation

[a] multiple-input multiple-output

Why SC-FDMA? - A PAPR-aware Transmitter

- Single-carrier vs. multi-carrier modulation?[a]
  - a PAPR[b] issue
  - OFDM[c]

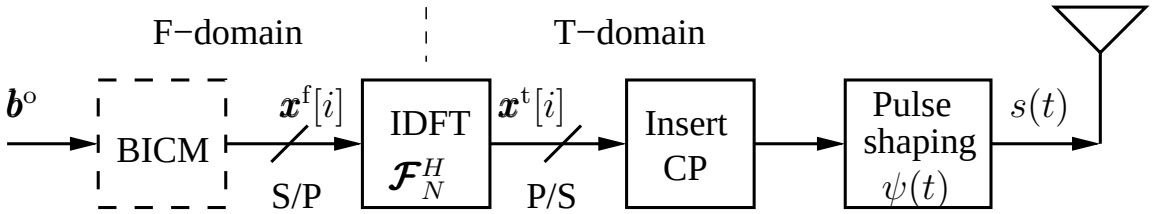

  - SC-FDE[d]

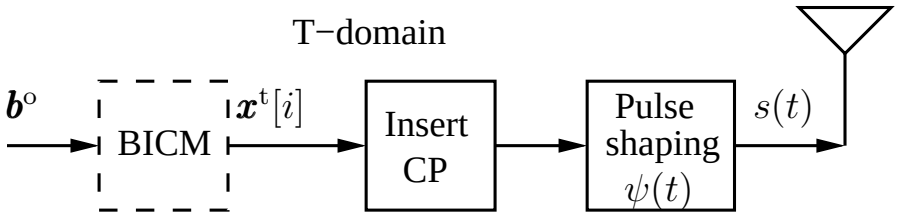

[a] *cyclic prefix* (CP) insertion, *forward error correction* (FEC) enabled by *bit-interleaved coded modulation* (BICM)
[b] peak-to-average power ratio
[c] orthogonal frequency-division multiplexing
[d] frequency-domain equalisation

Why SC-FDMA? - Complexity aware receiver design

- *Frequency-selective* fading – multi-path CIR[a]
- Conventional *time-domain* (TD) multi-tap equalisation

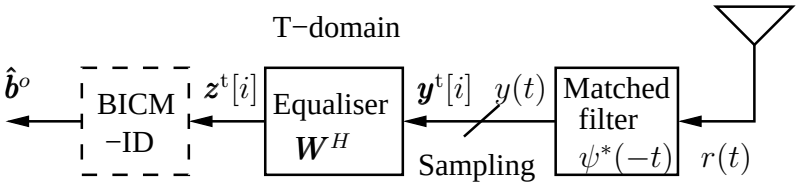

high complexity

- *Frequency-domain* (FD) single-tap equalisation

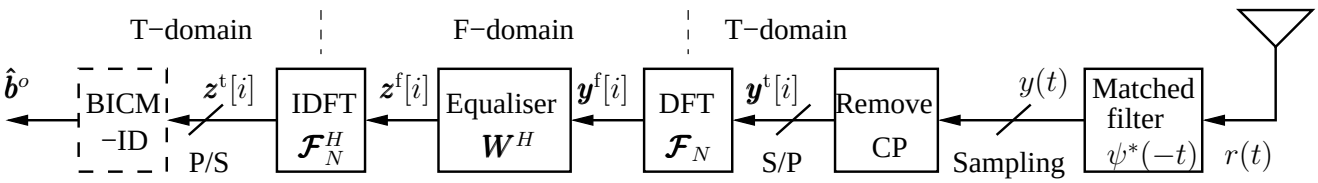

low complexity

[a] channel impulse response

Dynamic Resource Allocation for Opportunistic Relaying

Rationale: limited performance due to first-hop quality

Purpose: exploring extra selection diversity

Aspects: first-hop quality awareness

Objective: evaluate the advantages of joint design of

- dynamic relay selection (DRS)
- dynamic subband allocation (DSA)

Scope and Assumptions - Opportunistic Relay-aided Multi-user SC-FDMA Uplink

- Direct link is unavailable
- Relays geographically localised in a cluster at midway
- Cooperating relays are capable of exchanging CQI[a]
- BS's receiver employs multiple antennas

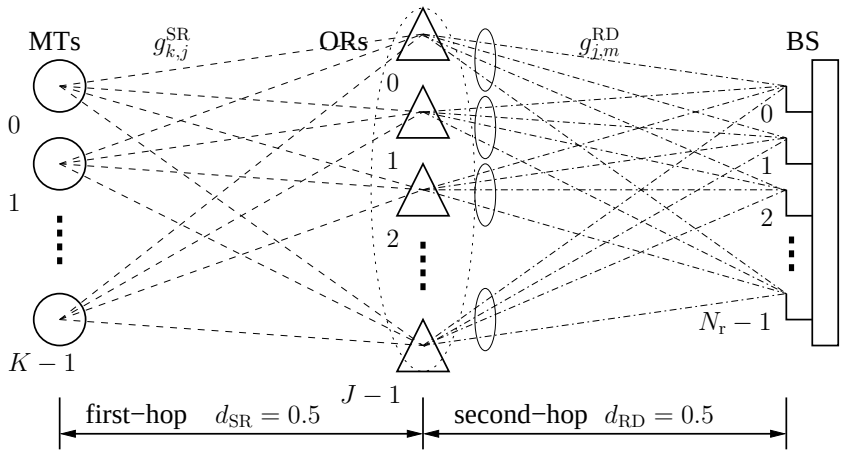

[a] channel quality information

Source/Relay Model - Multi-user Version

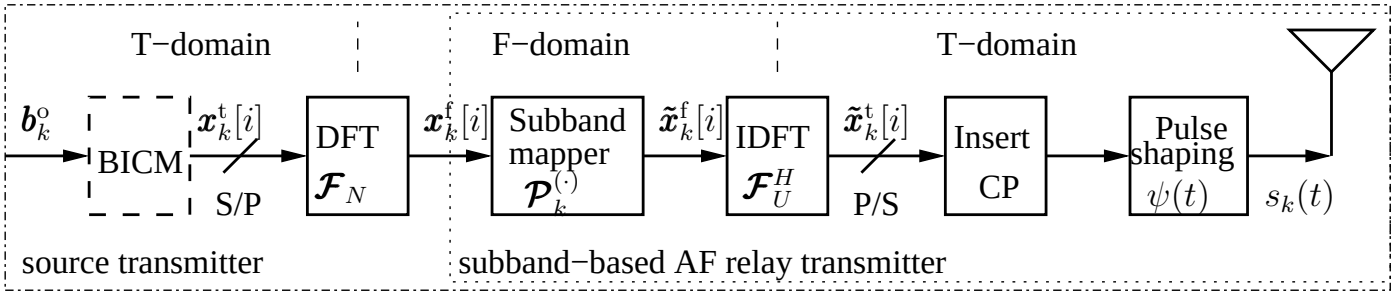

- K-user uplink, N subbands per user, U subbands in system
- N-point DFT-spreading $\mathcal{F}_N$, U-point IDFT-modulation $\mathcal{F}_U^H$
- bandwidth expansion factor M – full-load $K = M$
- Channel coded version: using *bit-interleaved coded modulation* (BICM)

Source/Relay Model - Multi-user Version

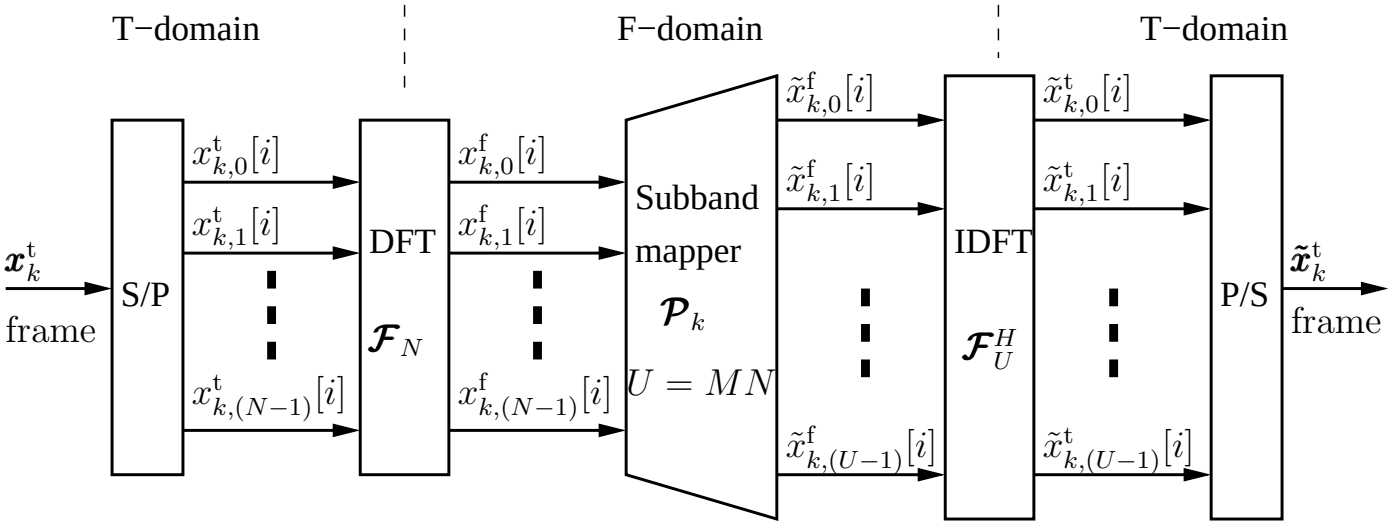

SC-FDMA Signalling - Symbol-to-subband Mapping

- Localised FDMA
  - block duration T_{v}, symbol duration T_{s}, chip duration T_{c}
  - user-specific *symbol-to-subband mapping* $\boldsymbol{\mathcal{P}}_k^{\mathrm{S}}$ for source or $\boldsymbol{\mathcal{P}}_k^{\mathrm{R}}$ for relay
- cyclic prefix (CP) insertion

TD signal waveform

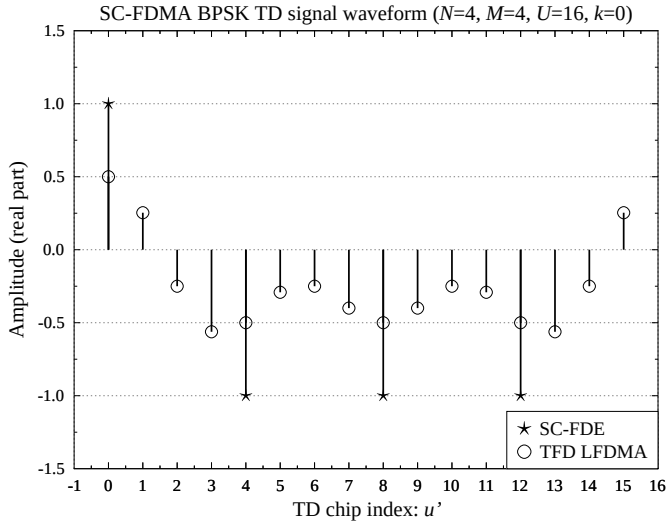

E.g. user $k = 0$, for $N = 4$,

$M = 4, U = 16$

FD subband mapping

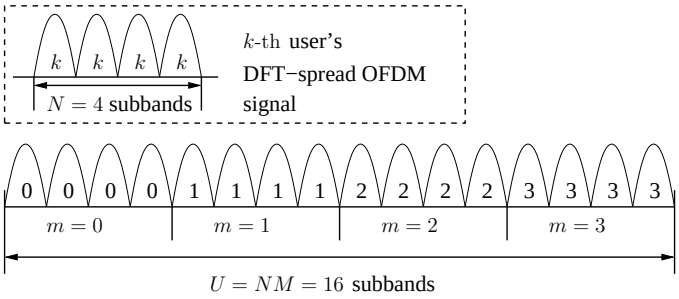

Relay/BS Receiver Model - Multi-user Version of SC-FDE Receiver

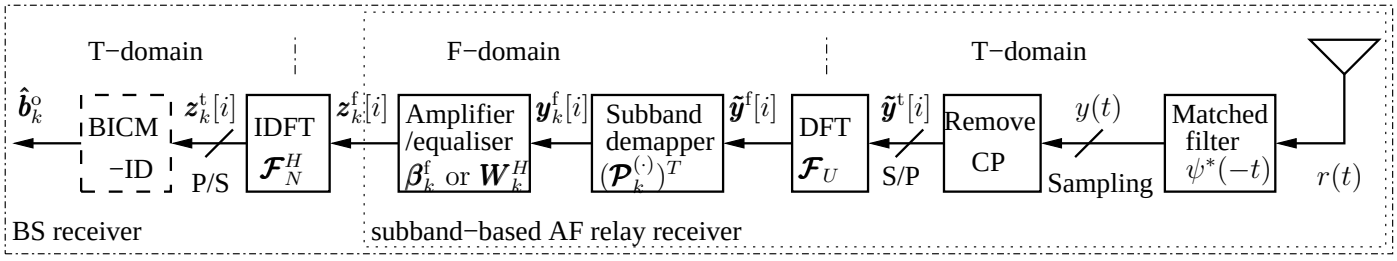

- subband demapping $\boldsymbol{\mathcal{P}}_k^{\mathrm{S}}$ at the relay or $\boldsymbol{\mathcal{P}}_k^{\mathrm{R}}$ at the BS
- relay: subband-based amplify-and-forward (AF) $\boldsymbol{\beta}_k^{\mathrm{f}}$
- BS: single-tap FDE $\boldsymbol{W}_k^H$ – diverse criteria[a]
- residual *inter-symbol interference* (ISI)

[a] *matched-filtering* (MF), *zero-forcing* (ZF) or *minimum mean-square-error* (MMSE)

Relay/BS Receiver Model - Multi-user Version

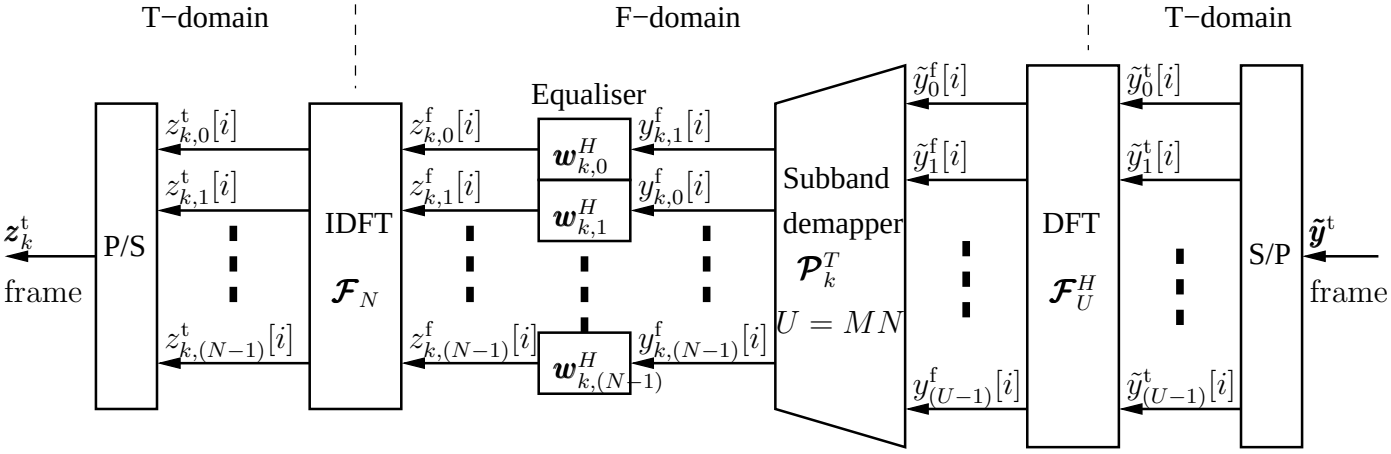

Dynamic Resource Allocation for Opportunistic Relaying

- Relay selection
  - *random relay selection* (RRS)
  - *dynamic relay selection* (DRS)
- Subband allocation
  - *static subband allocation* (SSA)
  - *dynamic subband allocation* (DSA)
- Dynamic resource allocation (DRA) for OR
  - conventional DRS combined with DSA (DRS-DSA)
  - first-hop-quality-aware joint DRA (FHQA JDRA)

    JDRA-1: dominated by the second-hop quality

    JDRA-2: dominated by the first-hop quality

Dynamic Resource Allocation - Comparisons

- Applied scenarios

Mode	Channel dependence	Relay strategy	Controller
DRS-SSA	R-D, low	Distributed non-coop.	BS
DRS-DSA	R-D, high	Localised non-coop.	BS
JDRA-1	S-R & R-D, high	Localised coop.	RCH[a]
JDRA-2	S-R & R-D, high	Localised coop.	RCH

- CQI exchange

Mode	Strategy	Context
JDRA-1	MWR[b]	S-R CQI order, and R-D CQI
JDRA-2	MWR	S-R CQI and R-D CQI

Dynamic Resource Allocation - Channel and Frame-structure

- Example of dynamic subband allocation for two users

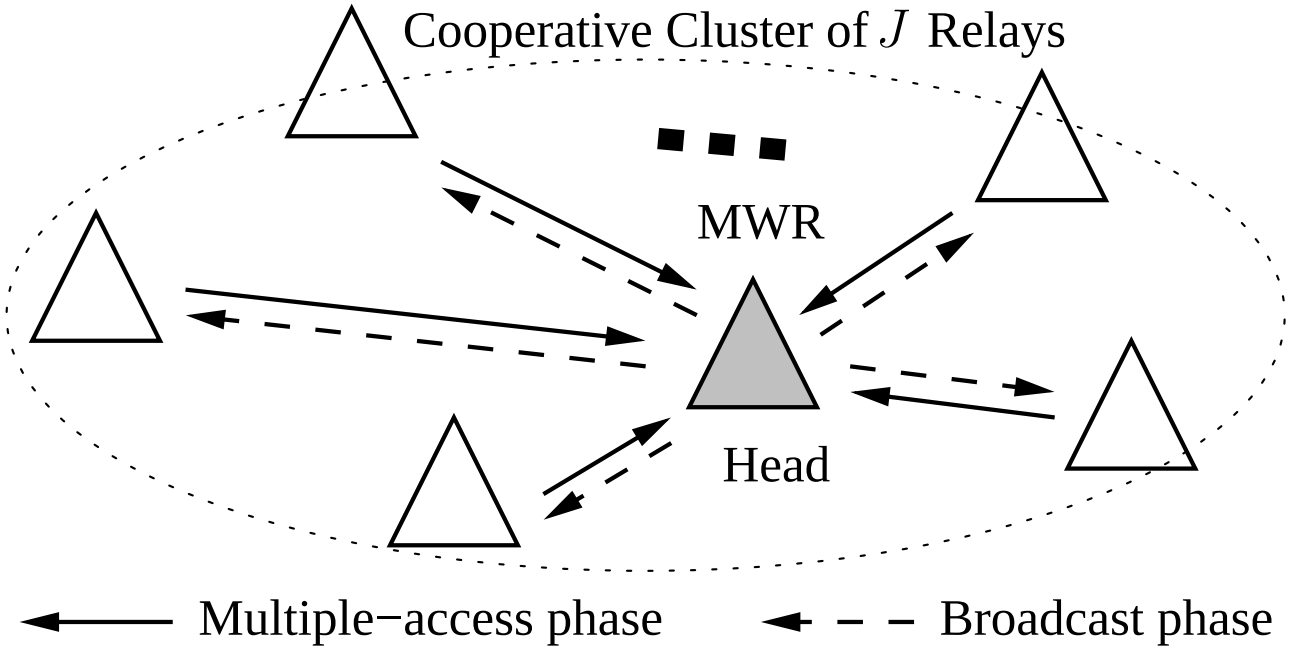

Dynamic Resource Allocation - Channel and Frame-structure

- Frame structure – resource vector (RV) and resource block (RB)

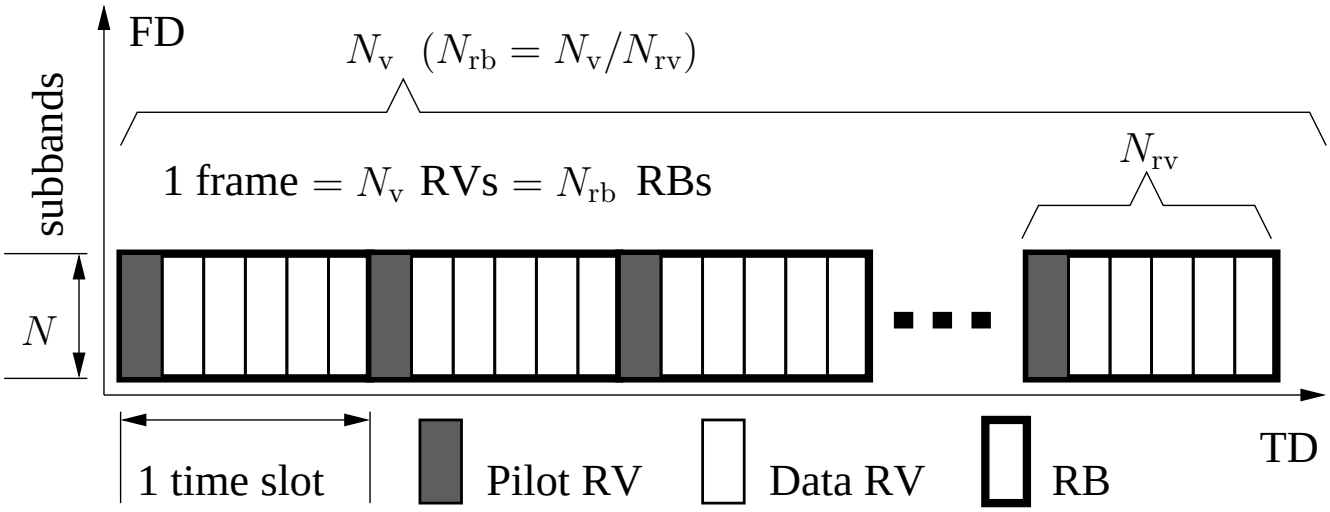

DRA - Conventional Schemes

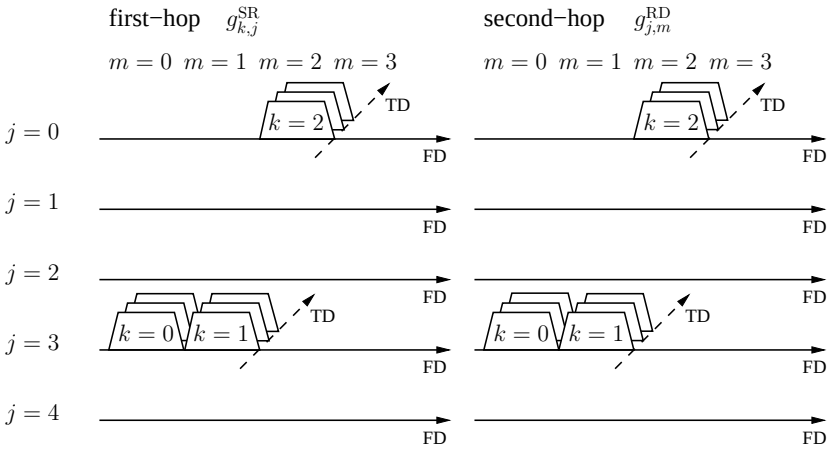

DRS-SSA

1. 2nd-hop DRS
2. 2nd-hop SSA
3. user assignment

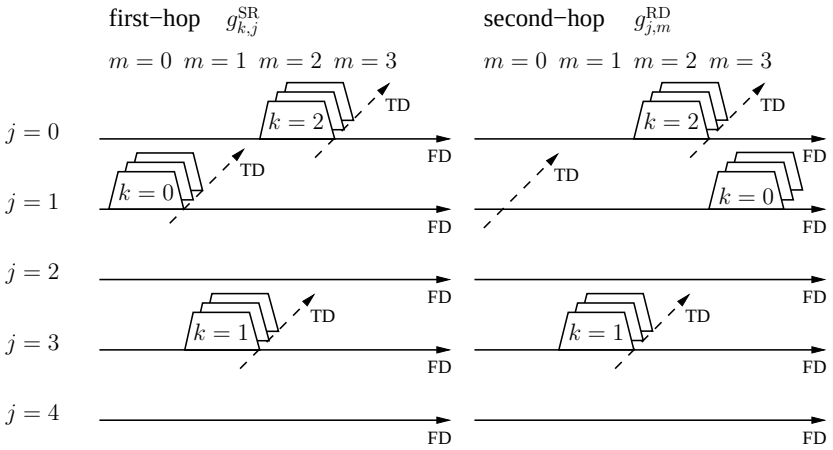

DRS-DSA

1. 2nd-hop DRS
2. 2nd-hop DSA
3. user assignment (randomly)

DRA - FHQA JDRA Schemes

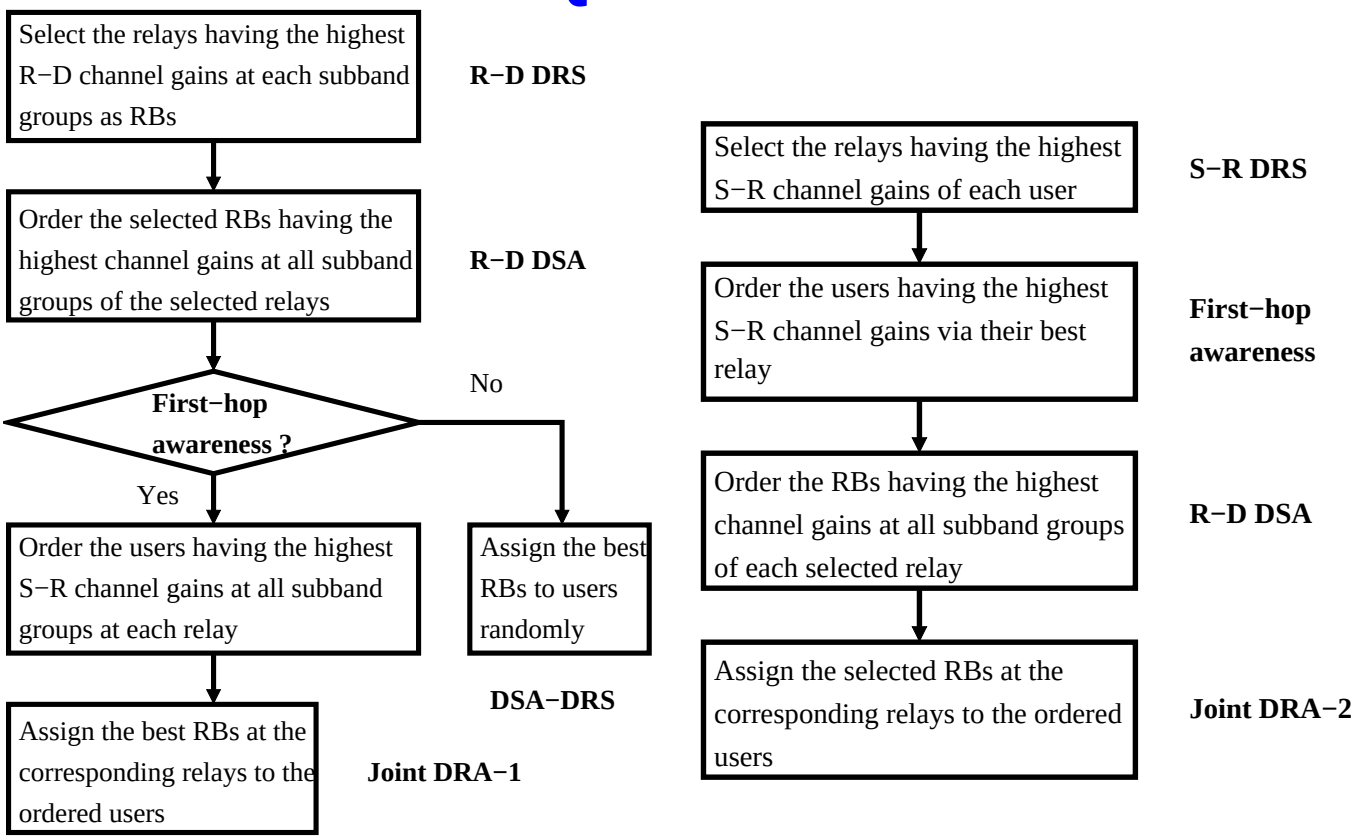

Parameters

S-D fading	no S-D link
S-R, R-D fading	frequency-selective Rayleigh
Power delay spread	uniform
Shadowing	absent ($\sigma_\xi^2 = 0$ dB)
Path-loss	$G_{\mathrm{SR}} = G_{\mathrm{RD}} = 0.5^{-4}$
Modulation	4-QAM (set-partitioning)
FEC coding	Non or RSC (2,1,3), $R_{\mathrm{c}} = 1/2$
Channel model	uncorrelated
Relaying protocol	amplify-and-forward (AF)
Relay selection	static or dynamic
Subband mapping	localised
Subband allocation	static or dynamic
Number of subbands per user	$N = 12$
Bandwidth expansion factor	$M = 6$
Total number of subbands	$U = 72$
Number of source users	$K = 6$
Number of paths	$L = 4$
Transmit power	$P_k^{\mathrm{S}} = P_k^{\mathrm{R}} = 0.5$
Number of BS receiver antennas	$N_{\mathrm{r}} = 1, 8$

BER vs. E_b/N_0
Uncoded OR SC-FDMA using MMSE FD-LE

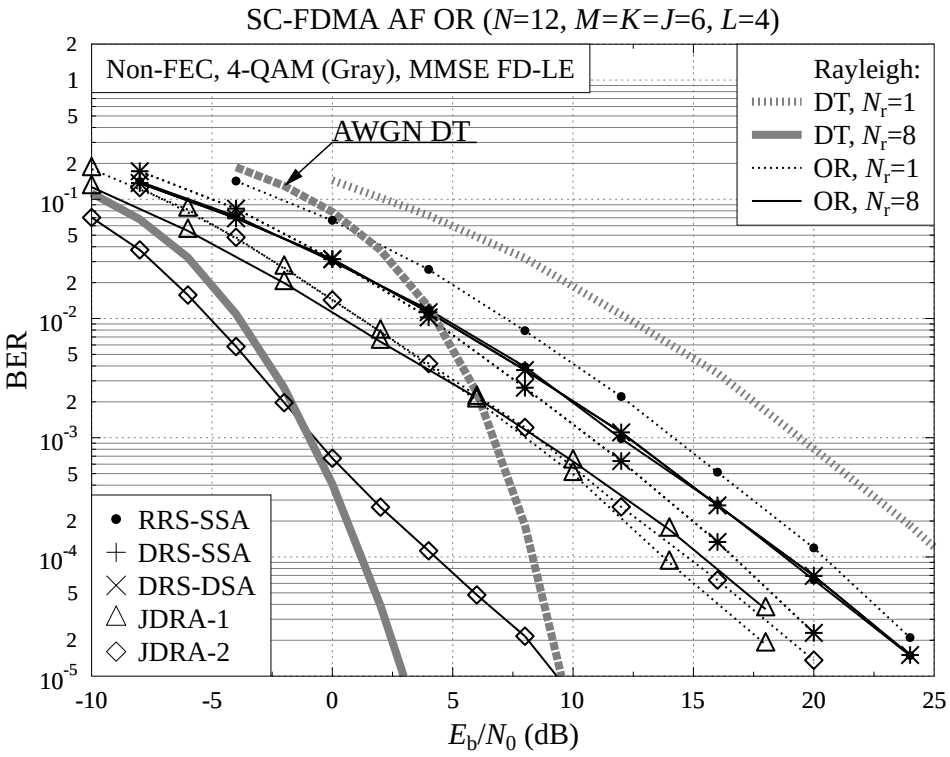

BER vs. E_b/N_0
Uncoded OR SC-FDMA using MMSE-SIC FD-DFE

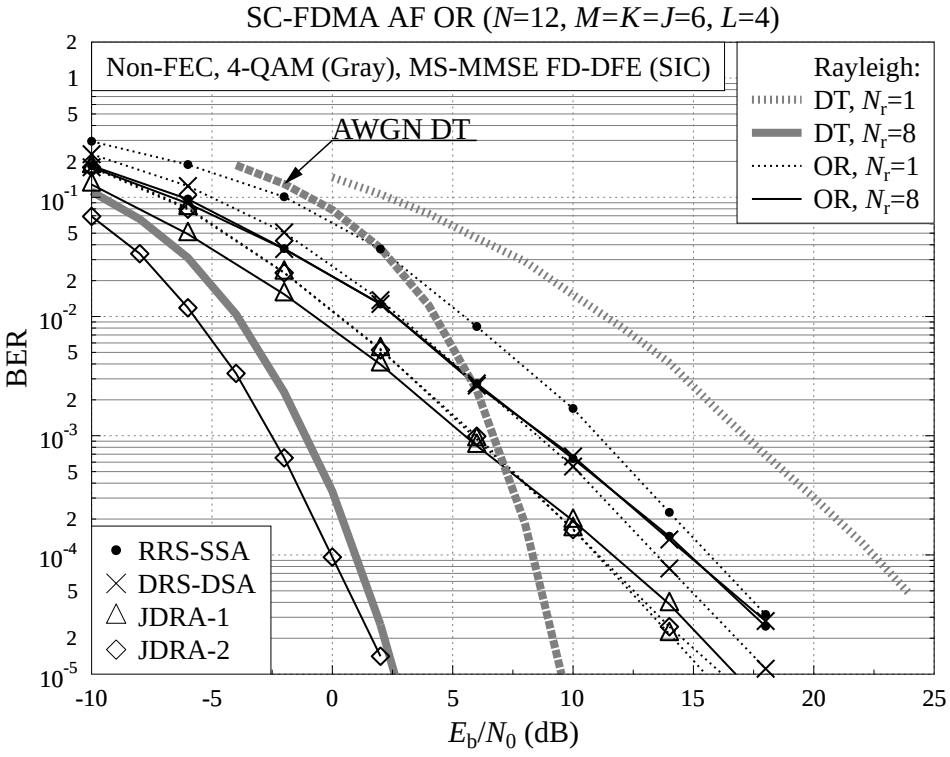

BER vs. E_b/N_0
BICM OR SC-FDMA using MMSE FD-LE

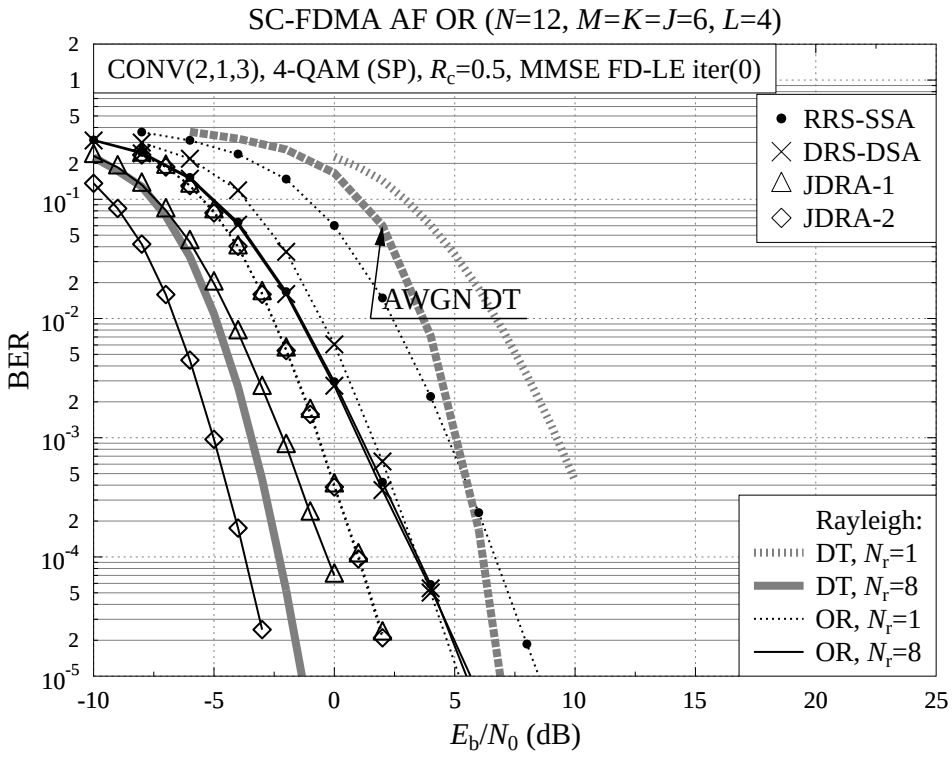

BER vs. the number of users K
Uncoded OR SC-FDMA using MMSE-SIC FD-DFE

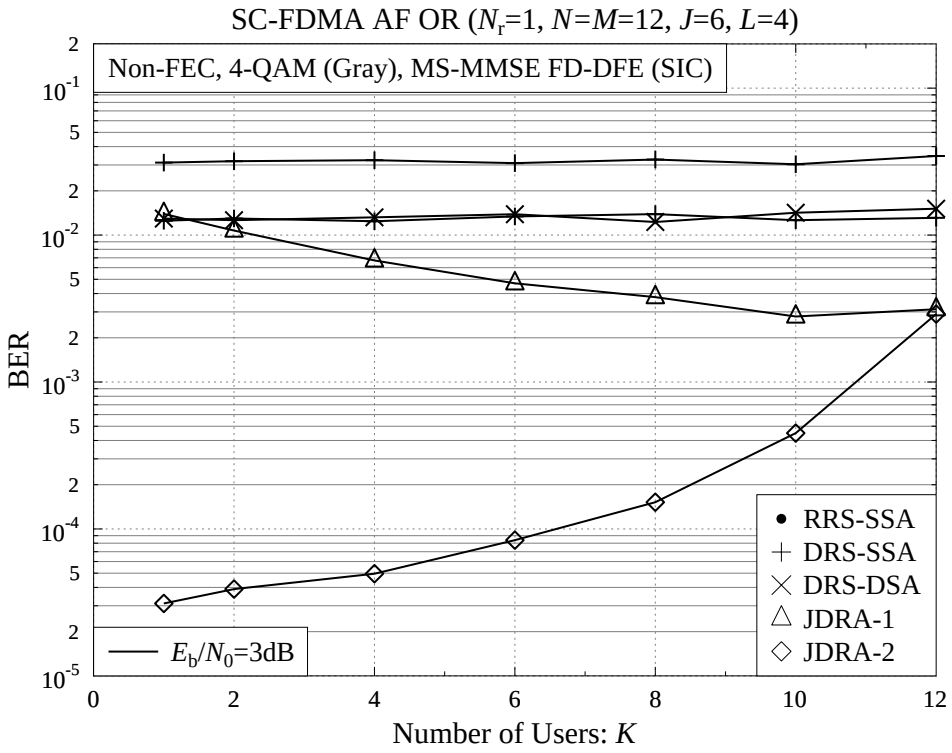

BER vs. the number of relays J
Uncoded OR SC-FDMA using MMSE-SIC FD-DFE

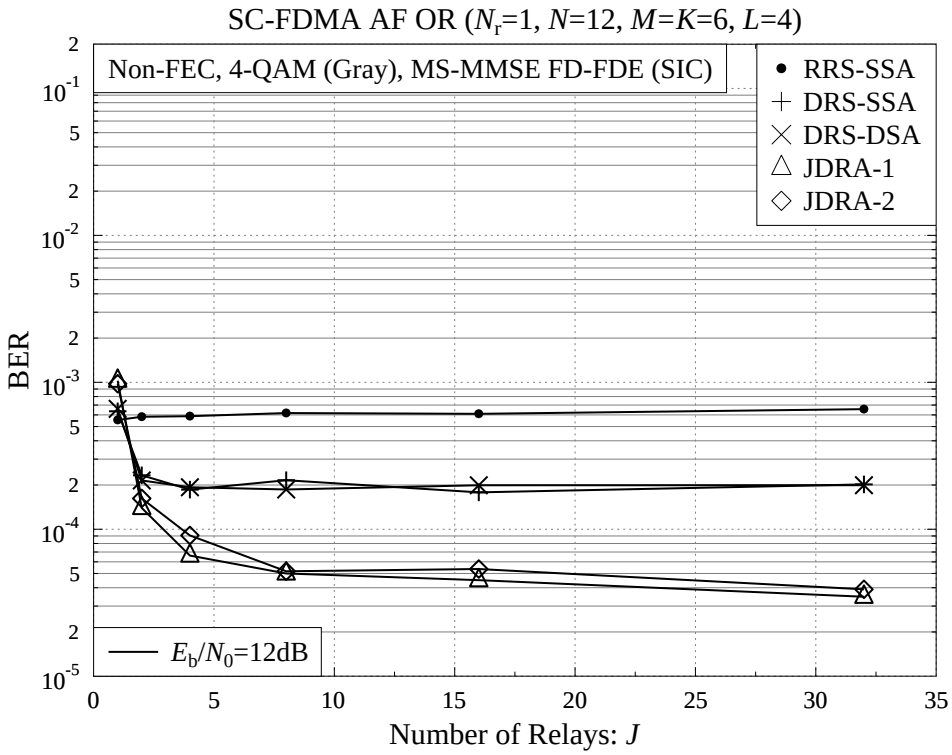

DRA-aided OR-based SC-FDMA Uplink vs. DT Benchmark

- Transmitted power reduction γ_b^{Δ} per bit may be achieved.
- The schemes are listed in descending order of complexity.

γ_b^{Δ} (dB)		Non-FEC		BICM	
	N_r	1	8	1	8
JDRA-2	AF	11.5	1	9.5	2
JDRA-1	AF	11.5	−11	9.5	−1
DRS-DSA	AF	8.5	−14	7.5	−3.5
RRS-SSA	AF	6.5	−14	5	−3.5

Conclusions

- We have: assumed that there are a number of inactive MTs acting as potential relays, which are geographically co-located in a cell;
- focused on the optimum exploitation of the relay selection and subband allocation for the two-hop transmissions;
- proposed two types of first-hop-quality-aware joint dynamic resource allocation schemes designed for the SC-FDMA uplink.

As a result, the reliability and power-efficiency of our proposed systems was significantly improved.

Future Work

In order to mitigate the inter-cell interference (ICI) and reduce the energy per bit in the multi-user multi-cell scenario, a trade-off has to be struck between the energy-efficiency and spectrum-efficiency at a system level.

- Relay-assisted multi-cell resource allocation
- Link-quality-aware relay-assisted network optimisation

IEEE Wireless Communications and Networking Conference 2012

Paris, France

Effects of Practical Impairments on Cooperative Distributed Antennas Combined with Fractional Frequency Reuse

Jie Zhang, Rong Zhang, Xinyi Xu, Guangjun Li, Lajos Hanzo

Communications Research Group

School of Electronics and Computer Science

University of Southampton, UK.

Email: {jz4, rz, lh}@ecs.soton.ac.uk

http://www-mobile.ecs.soton.ac.uk

Outline

- ❏ System model
- ❏ Assumptions
- ❏ Precoding
- ❏ Practical impairments
- ❏ Synchronisation errors
- ❏ Results and discussions
- ❏ Conclusions

Key References

- M. Sadek and A. Tarighat and A. H. Sayed “A leakage-based precoding scheme for downlink multi-user MIMO channels”, *IEEE Transactions on Wireless Communications*, vol.55, no. 5, pp. 1711–1721, May 2007.
- M. Speth and S. A. Fechtel and G. Fock and H. Meyr “Optimum receiver design for wireless broad-band systems using OFDM - Part I”, *IEEE Transactions on Communications*, vol. 47, no. 11, pp. 1668–1677, Nov. 1999.
- X. Xu and R. Zhang and S. Ghafoor and L. Hanzo, “Imperfect Digital-Fibre-Optic-Link-Based Cooperative Distributed Antennas With Fractional Frequency Reuse in Multicell Multiuser Networks”, *IEEE Transactions on Vehicular Technology*, vol. 60, no. 9, pp. 4439–4449, Nov. 2011.

Motivation

- High Frequency Reuse (FR) Factor:
  - low spectral efficiency but high SINR at the cell-edge
- Received signal and SINR

$$y_j = h_{0,j}x_j + \sum_{i\in\mathbb{B}} h_{i,j}x_i + n_j$$

$$\gamma_j = \frac{|h_{0,j}|^2}{|n_j|^2 + \sum_{i\in\mathbb{B}}|h_{i,j}|^2}$$

  - $\mathbb{B} = \{B_i, i \in 8, 10, \cdots, 18\}$

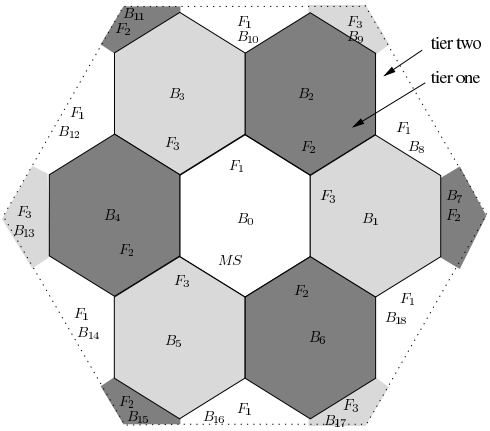

FR transmission

- Unity Frequency Reuse (UFR)
  - high spectral efficiency but low SINR at the cell-edge
- Received signal and SINR

$$y_j = h_{0,j}x_j + \sum_{i\in\mathbb{B}_o} h_{i,j}x_i + n_j$$

$$\gamma_j = \frac{|h_{0,j}|^2}{|n_j|^2 + \sum_{i\in\mathbb{B}_o}|h_{i,j}|^2}$$

  - $\mathbb{B}_o = \{B_i, i \in 1,2,\cdots,18\}$

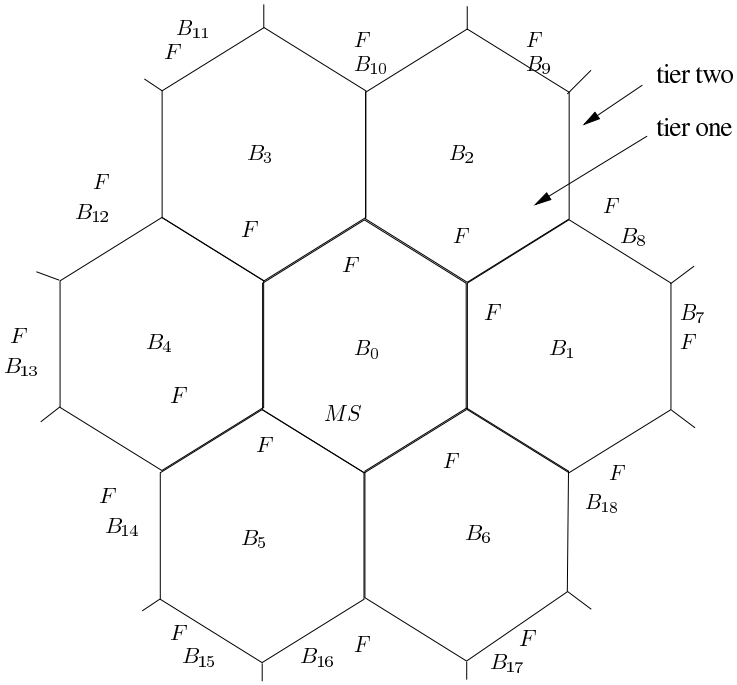

UFR transmission

- Fractional Frequency Reuse (FFR)
  - high SINR at the cell-edge but reduced spectral efficiency
- Received signal and SINR at cell-edge is the same as that of FR transmission
- Received signal and SINR at cell-centre is the same as that of UFR transmission

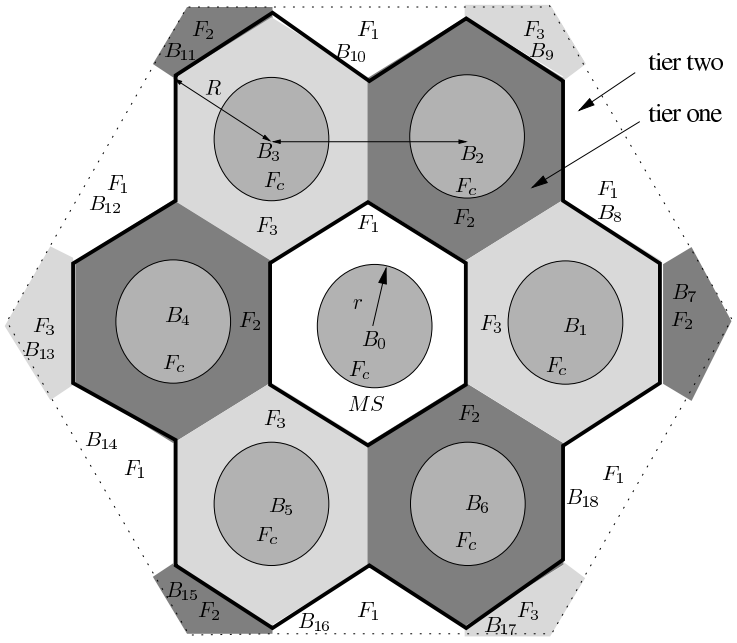

FFR transmission

- Distributed Antenna System (DAS) aided FFR Transmission
  - *spatial diversity gain, mitigates the pathloss and large-scale fading*
  - high SINR and high spectral efficiency
- Received signal and SINR at the cell-edge

$$y_j = h_{j,j}x_j + \sum_{i=1,i\neq j}^{N_a} h_{i,j}x_i + n_j^*$$

$$\gamma_j = \frac{|h_{j,j}|^2}{|n_j^*|^2 + \sum_{i=1,i\neq j}^{N_a}|h_{i,j}|^2}$$

  - $n_j^* = n_j + \sum_{i\in\mathbb{B}} h_{i,j}x_i$ denotes the AWGN and the CCI from tire-two cells.

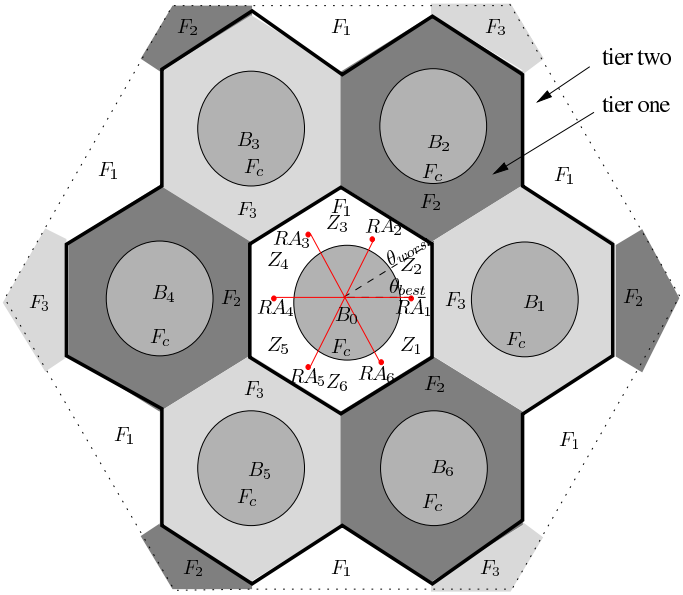

FFR-DAS transmission

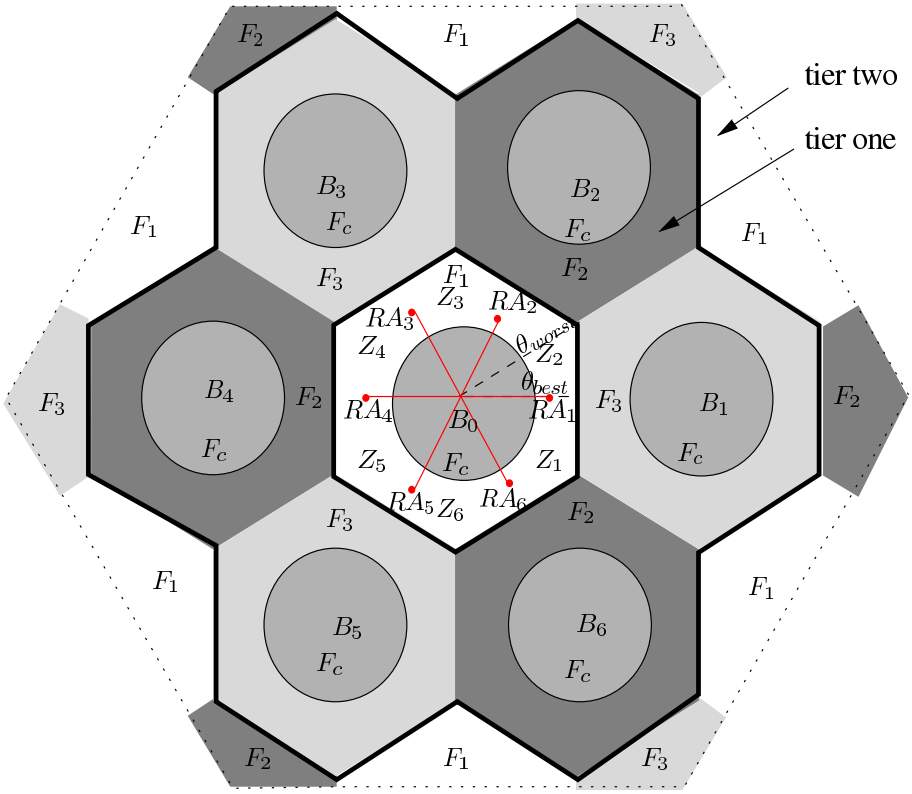

NonCoMP-aided FFR-DAS transmission

Non-Cooperative DAS-aided FFR DL transmission?

- FFR-DAS transmission is capable of providing
  - N_a hot spots around the N_a DAs
  - Path loss gain
  - Spatial diversity gain

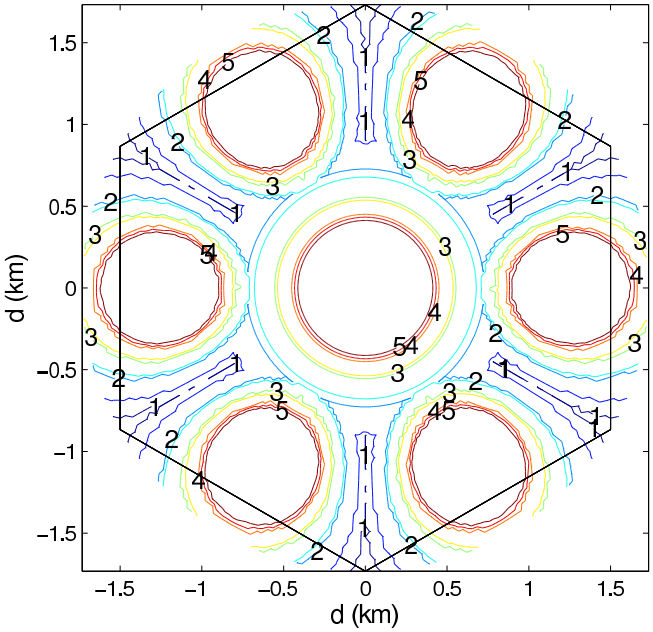

Throughput of DAS-aided FFR transmission without CoMP

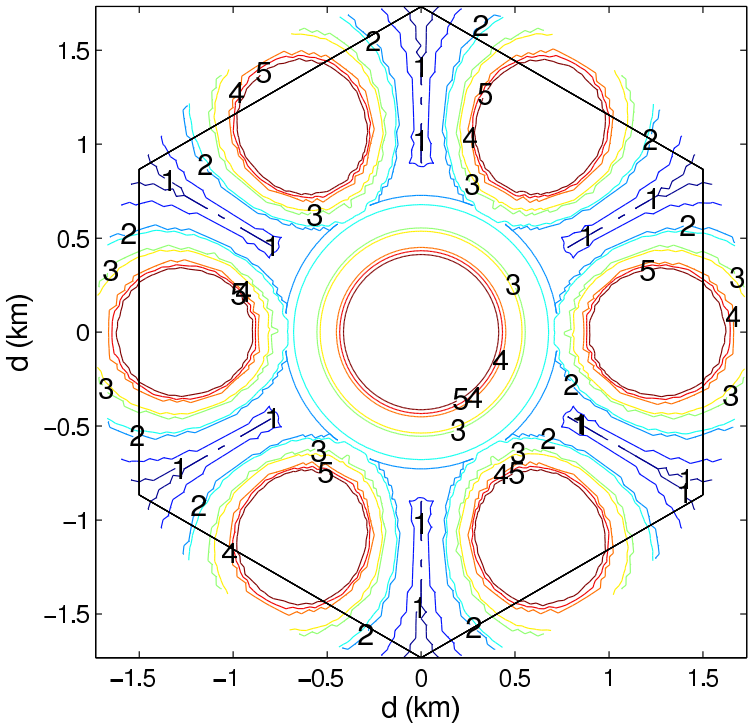

Throughput of FFR-DAS transmission without CoMP

Why cooperative?

- Reason
  - Strong CCI for users roaming near the angle halfway between the adjacent DAs for the Non-CoMP aided FFR-DAS.
- Benefits of CoMP
  - Increasing system throughput
  - Extending cellular coverage
  - Supports multiple users
- Requirement
  - full Channel State Information (CSI) at all BSs

CoMP-aided FFR-DAS DL transmission

- Configure
  - 6 DAs act as a distributed BS
  - Supports $N_u = 6$ users simultaneously
- Received signal and corresponding SINR

$$y_j = \mathbf{h}_j \mathbf{t}_j x_j + \sum_{i=1, i \neq j}^{N_u} \mathbf{h}_j \mathbf{t}_i x_i + n_j^*$$

$$\gamma_j = \frac{|\mathbf{h}_j \mathbf{t}_j|^2}{|n_j^*|^2 + \sum_{i=1, i \neq j}^{N_u} |\mathbf{h}_j \mathbf{t}_i|^2}$$

  - $\mathbf{t}_j$ - precoding vector for MS j employed at transmitter.

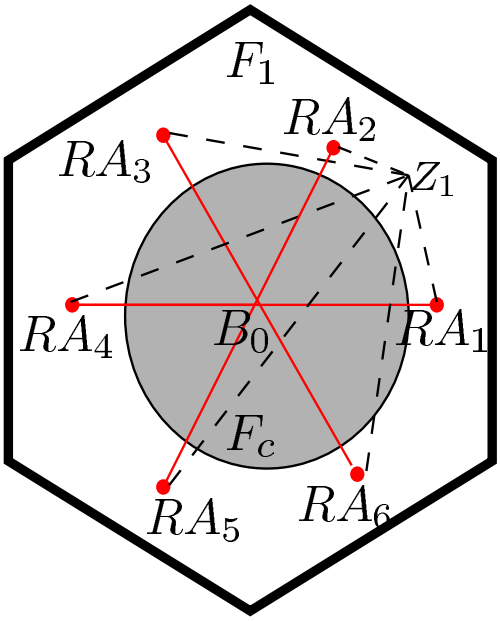

CoMP-aided FFR-DAS

Assumptions

- MS located at the angle halfway between DAs.
- The DL signal destined for the MSs is perfectly received from the BS at the DAs.
- Complex-valued additive white Gaussian noise (AWGN) $\mathcal{CN}(0, N_0)$ at the MS
- Single receive antenna at each MS.
- Single DL transmit antennas at both the BS and the DAs.

Signal-to-Interference-Leakage-plus-Noise-Ratio (SILNR) DL Precoding

- Aims for
  - Maximising the SILNR for the intended MS.
  - Minimising the leakage interference imposed on other MSs
- SILNR expresion

$$\eta_{i,j} = \frac{|\mathbf{h}_{i,j}\mathbf{t}_{i,j}|^2}{\sum_{k=1,k\neq j}^{N_u}|\mathbf{h}_{i,k}\mathbf{t}_{i,j}|^2 + N_0/P_{i,j}}$$

  - $\mathbf{h}_{i,j}$ – channel vector between the DA i and the MS j
  - $\mathbf{t}_{i,j}$ – Precoding vector at DA i for transmitting the jth MS's signal.
  - $P_{i,j}$ – Transmission power at DA i for MS j.

Signal-to-Interference-Leakage-plus-Noise-Ratio (SILNR) DL Precoding

❑ Proportional power allocation strategy

$$P_{i,j} = \frac{|\mathbf{h}_{i,j}|^2}{\sum_{i,k=1}^{N_u} |\mathbf{h}_{i,k}|^2} P_i$$

- $P_{i,j}$ – power allocated for the jth MS at DA i
- P_i – available power at DA i

❑ Solution

$$\mathbf{t}_{i,j} = \text{max. eigv}[(N_0/P_{i,j} + \sum_{k=1,k\neq j}^{N_u} \mathbf{h}_{i,k}^H \mathbf{h}_{i,k})^{-1} \mathbf{h}_{i,j}^H \mathbf{h}_{i,j}]$$

- $\mathbf{t}_{i,j}$ is multiplied by the allocated power $P_{i,j}$.

CSI Imperfection: Estimation errors

❑ Channel at MS j with CSI estimation errors

$$\mathbf{h}_j = \hat{\mathbf{h}}_j + \mathbf{e}_j$$

- $\mathbf{e}_j$ - Additive Gaussian noise at the jth MS having variance of σ_e^2.
- $\hat{\mathbf{h}}_j$ - The estimated channel at the jth MS with variance of $1 - \sigma_e^2$.

❑ The model is also suitable for other CSI errors, such as the CSI feedback delay.

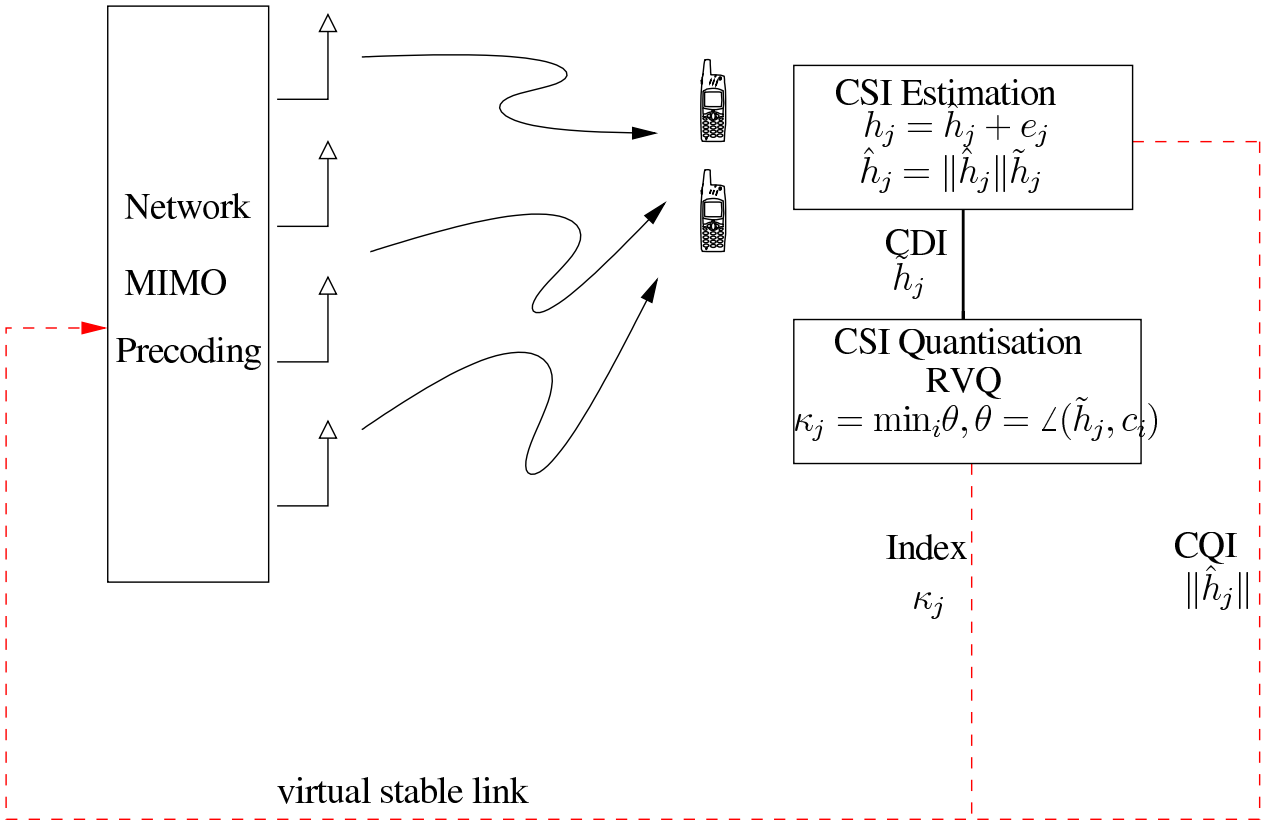

CSI feedback model

CSI Imperfection: Quantisation

❑ Quantisation channel model

$$\hat{\mathbf{h}}_j = \|\hat{\mathbf{h}}_j\| \cdot \tilde{\mathbf{h}}_j$$

- $\|\hat{\mathbf{h}}_j\|$ - Channel Quality Information (CQI).
- $\tilde{\mathbf{h}}_j$ - Channel Direction Information (CDI).

❑ Assumption

- $\mathbf{C} = \{\mathbf{c}_1, \mathbf{c}_2, \cdots, \mathbf{c}_{2^b}\}$ - Codebook having 2^b entries is pre-designed and it is available to both the MS and the BS.
- CQI $\|\hat{\mathbf{h}}_j\|$ and quantisation index κ_j are perfectly fed back to the BS.

❑ Random Vector Quantisation (RVQ)

- Codebook element $\mathbf{c}_i$ is a randomly generated zero-mean, unity-norm Gaussian vector.
- The quantisation index $\kappa_j = \max_{i=1,2,\cdots,2^b} \cos\theta, \theta = \angle(\tilde{\mathbf{h}}_j, \mathbf{c}_i)$.

Synchronisation errors

- Time offset: The Inter-Symbol-Interference (ISI) imposed by the time offset is treated as additive noise n_ε with a variance of

$$\sigma_\varepsilon^2 = \sum_m |\mathbf{h}_j(\tau_m)|^2 [2\frac{\Delta\varepsilon_m}{N} - (\frac{\Delta\varepsilon_m}{N})^2]$$

- Frequency offset $\phi = \frac{\Delta f}{1/T_u}$: Similar to the time-offset errors, the FD cross talk (ICI) is also treated as additive noise n_Ω having a variance of

$$\sigma_\Omega^2 \approx \frac{\pi^2}{3}\phi^2$$

- Both the time offset as well as the frequency offset errors will degrade the received SINR at the MS.

Worst-Case-Angle Results & Discussions

❑ Achievable SINR as a function of Tx SNR with imperfect CSI

- Highest SINR is achieved by FFR transmission at high Tx SNR.
- SINR of CoMP transmission under perfect CSI outperforms the UFR and FFR benchmarkers.
- CoMP transmission degrades at low quantisation quality.

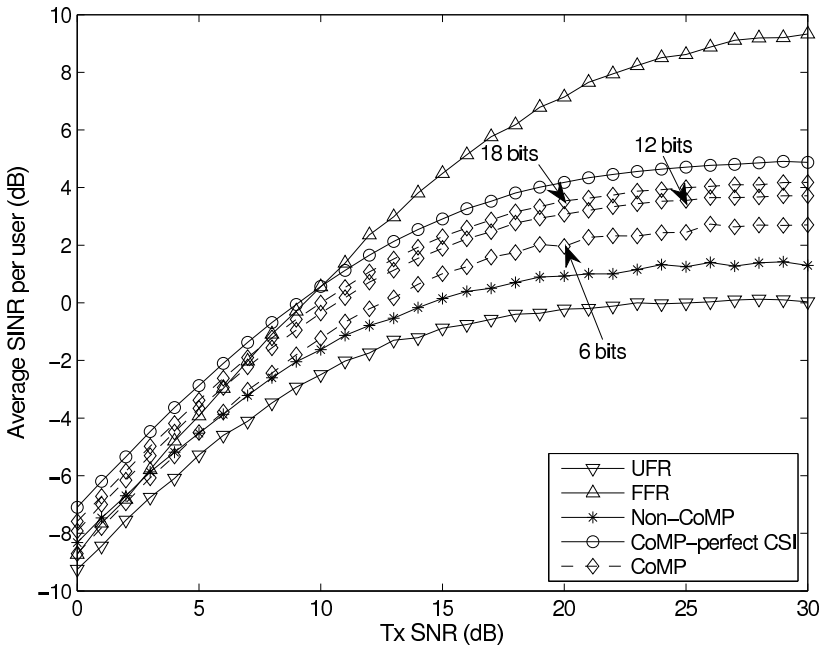

- SINR of CoMP-FFR under both imperfect CSI as well as a synchronisation error of **0.2 x CP=0.2 x 72**
  - Achievable SINR becomes worse than that of NonCoMP transmission at low SNR, when synchronisation errors and CDI quantisation errors coexists.

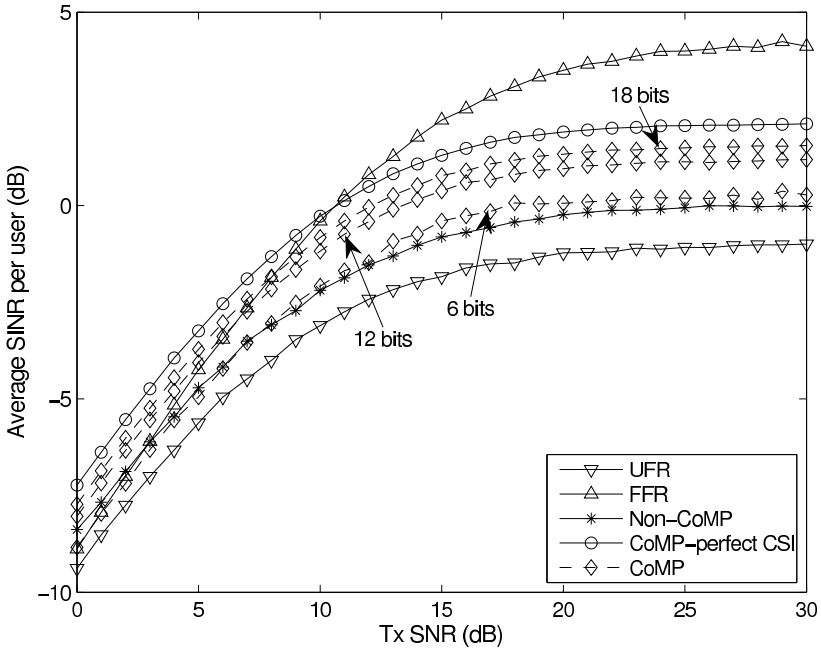

- SINR loss at different time offsets (CP=72)
  - Highest SINR loss for FFR transmission
  - Similar SINR loss for idealised and practical CoMP transmission.
  - Small SINR loss for Non-CoMP and UFR

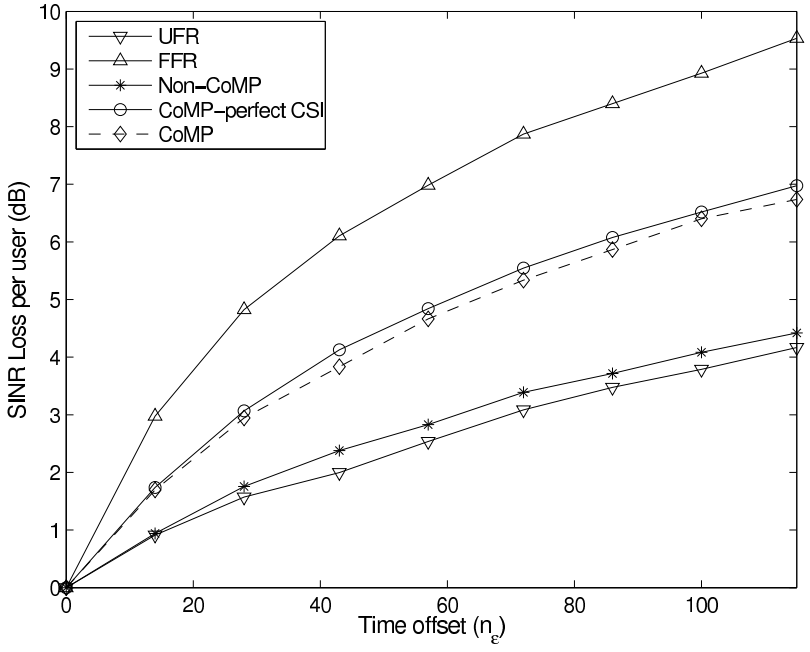

- SINR loss for different frequency offsets
  - Similar trends to those of time offsets
  - But more sensitive to frequency errors than to time offsets.

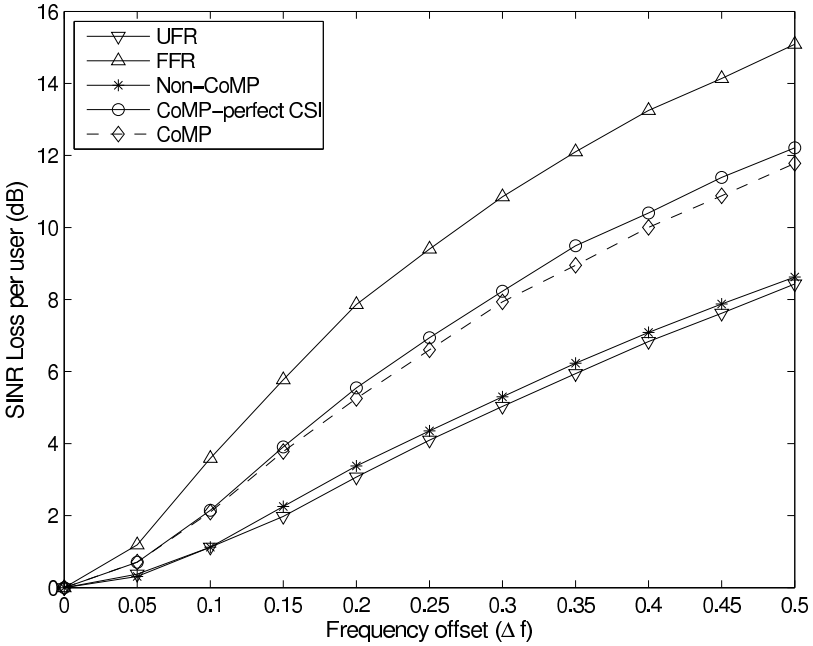

Conclusions

- CoMP-aided FFR-DAS was studied for imperfect CSI and synchronisation errors, when the MS is located at half the angle between the DAs
  - SILNR precoding technique was employed.
  - Practical CSI errors as well as synchronisation errors were considered.
  - Higher SINR for CoMP transmission for both imperfect CSI as well as for synchronisation errors.
  - More sensitive to frequency offsets than that to time offsets.

Future Research

- Near-capacity multi-functional MIMO arrays supporting diverse non-coherent detection aided asynchronously detected wireless tranceivers.
- Cross-layer designed assisted 'green' wireless systems

Thank You